2019

EFFECTS OF INVASIVE WATERMILFOIL AND SEASONAL DYNAMICS ON PRIMARY PRODUCTION IN LITTORAL ZONES OF NORTH-TEMPERATE LAKES

Ryan R. Van Goethem
Michigan Technological University, rrvangoe@mtu.edu

EFFECTS OF INVASIVE WATERMILFOIL AND SEASONAL DYNAMICS ON PRIMARY PRODUCTION IN LITTORAL ZONES OF NORTH-TEMPERATE LAKES

By

Ryan R. Van Goethem

A THESIS

Submitted in partial fulfillment of the requirements for the degree of

MASTER OF SCIENCE

In Biological Sciences

MICHIGAN TECHNOLOGICAL UNIVERSITY

2019

This thesis has been approved in partial fulfillment of the requirements for the Degree of MASTER OF SCIENCE in Biological Sciences.

Department of Biological Sciences

Thesis Advisor:	*Dr. Amy Marcarelli*
Committee Member:	*Dr. Casey Huckins*
Committee Member:	*Dr. Molly Cavaleri*
Department Chair:	*Dr. Chandrashekhar P. Joshi*

Table of Contents

Author Contribution Statement

This thesis was written in 2 separate chapters. The first chapter will be submitted for publication in the scientific journal *Biological Invasions* with coauthors Amy M. Marcarelli and Casey J Huckins. For both chapters, the project design, funding, and writing were completed in collaboration with Amy M. Marcarelli at Michigan Technological University. I led execution of the research, which included protocol and gear development, field data collection, laboratory analysis, data analysis, and writing.

Acknowledgements

This research was funded by the Midwest Aquatic Plant Management Society Robert L. Johnson Memorial Grant, Michigan Chapter of North American Lake Management Society, Society for Freshwater Science, and Michigan Technological University. Valuable experience and financial support for my education came from US EPA Great Lake Restoration Initiative project (GL-00301928-0) and Michigan Invasive Species Grant Program (#IS14-2005). I would also like to thank the Department of Biological Sciences by funding through teaching assistantships.

I would like to thank my advisor, Dr. Amy Marcarelli for her mentorship and support through my education as I have learned an enormous amount of science, writing, and effective communication on this adventure. I would also like to acknowledge my committee members Dr. Casey Huckins and Dr. Molly Cavaleri for feedback and comments which helped my project. I gained bountiful experience and financial support while working with Colin Brooks in the field as part of the Great Lakes Restoration Initiative project. I would like to thank members of our lab, Kevin Nevorski, Erin Eberhard, and Joslyn Pomeroy as they helped on numerous occasions collect samples during arduous field days and perform lab analyses. Thank you also Meredith Brehob, Renn Schipper, Rylie Kostreva, Andie Norton, Samantha Doyle and Maya Brayden with help lab analyses and sample processing. I want to thank my family and friends for giving me the support and encouragement to see my graduate degree to its conclusion. And lastly, I would

love to thank my fiancée Lauren Grzelak, who has always been there to motivate and support me through graduate school and writing this thesis.

Abstract

Climate change and species invasion are two agents of global change altering aquatic ecosystems worldwide. Submerged aquatic macrophytes control lake ecosystem processes through their direct and indirect interactions with other primary producers, but how their interactions may be altered by species invasions or how they function over full seasonal cycles in temperate lakes is poorly understood. We first addressed whether the presence of invasive watermilfoil (IWM) altered standing crops and gross primary production (GPP) of other littoral primary producers (macrophytes, phytoplankton, attached algae or periphyton) in littoral zones of 6 Michigan lakes. We found no differences in primary producer standing crops or GPP between plots with or without IWM. Macrophyte standing crop predicted rates of benthic periphyton GPP and standing crops of all other primary producers across all study plots, along with water temperature, nutrient concentrations, and water clarity. Second, we studied year-round dynamics of littoral primary producers in 2 lakes located on the Keweenaw Peninsula of the Upper Peninsula of Michigan. Standing crops of primary producers were present all year and changed seasonally, although they were lowest during winter. Water temperature explained 34% of phytoplankton GPP and 57% of plot-level GPP, which incorporated all primary producers. Water under the ice was hypoxic during winter. Together, the results of these studies suggest that macrophyte biomass, temperature and ice cover are important drivers of littoral zone productivity among lakes and over seasons, which has implications for understanding possible effects of climate change on ecosystem processes in north temperate lakes.

1 Effects of Invasive Watermilfoil on Primary Production in Littoral Zones of North-Temperate Lakes

1.1 Introduction

Eurasian watermilfoil (*Myriophyllum spicatum*) is an invasive aquatic macrophyte which has spread across the contiguous United States over the past century (Smith and Barko 1990) from source populations traced back to Asia (Moody et al. 2016). Eurasian watermilfoil invades the shallow water habitat of lakes, called littoral zones, where it can grow rapidly and build a canopy, suppressing other aquatic plants (macrophytes) below (Madsen et al. 1991; Boylen et al. 1999). Although Eurasian watermilfoil is perennial, it exhibits an annual pattern of growth where in the spring shoots grow rapidly to the water's surface, then branch profusely throughout the growing season (Madsen and Boylen 1989). Plants remain evergreen in the fall and overwinter with substantial biomass, allowing them to grow rapidly in the spring to establish dominance early in the next growing season (Nichol and Shaw 1986). Vegetative reproduction and dispersal of fragments is the primary vector of spread within and between waterbodies (Smith and Barko 1990). Eurasian watermilfoil can hybridize with native Northern watermilfoil (*M. sibiricum*) to create hybrids (*Myriophyllum spicatum* x *sibiricum*) that exhibit increased growth vigor and increased resistance or tolerance to herbicides (Larue et al. 2013; Parks et al. 2017; Thum et al. 2017). Pure Eurasian watermilfoil and its hybrids are invasive, present in Michigan (Moody and Les 2007), and difficult to differentiate visually (Parkinson et al. 2011), so will be considered collectively in this study as invasive watermilfoil (IWM).

Dense, high biomass growths of IWM can cause deleterious effects to waterbodies by inhibiting recreational access and opportunities, along with altering populations of macroinvertebrates and fishes (Smith and Barko 1990) and energy flow in lake food webs (Kovalenko and Dibble 2014). These same dense patches of IWM interact with all other primary producers in the littoral zone, with potential consequences for their distribution and production.

Submerged macrophytes directly and indirectly interact with other primary producers in lake littoral zone, and through these interactions can control lake ecosystem processes (Carpenter and Lodge 1986). In a study of lakes in Wisconsin, areas of littoral habitats with high macrophyte abundance contributed disproportionately to whole lake primary production, while those with low abundance of macrophytes had similar primary production as open water (pelagic) habitats (Lauster et al. 2006). Macrophytes create structure and substratum while also modifying light and nutrient dynamics, all of which can interact to affect other littoral primary producers (Figure 1.1). Macrophyte vegetative structure and leaf area limit light penetration in the water column and to the lake bottom (Binzer et al. 2006), which can reduce light availability for phytoplankton (free floating single cell and colonial algae), epiphytes (attached algae growing on macrophytes), and benthic periphyton (attached algae growing on bottom substrata). Macrophytes primarily take up nutrients from the sediment and are capable of large reductions in sediment pools of nitrogen and phosphorus (Barko et al. 1988), yet also use inorganic nutrients from the water column (Cattaneo and Kalff 1980; Barko and Smart 1981). In contrast, phytoplank-

ton have high affinity for dissolved nutrients and primarily obtain nutrients from the water column (Reuter and Axler 1992; Vadeboncoeur and Steinman 2002). Epiphytes and benthic periphyton have access to nutrients from their substratum, the water column, and internal recycling within any biofilm matrix (Carignan and Kalff 1982; Vadeboncoeur et al. 2006). When large amounts of dissolved nutrients are available in eutrophic lakes, phytoplankton standing crops increase, which induces stronger light limitation of benthic periphyton (Vadeboncoeur et al. 2001), epiphytes and macrophytes (Scheffer et al. 1993). Further complicating interactions, epiphytes can take advantage of higher light intensities available at elevated positions in the water column from macrophytes, while also obtaining nutrients released by the macrophytes (Carignan and Kalff 1982; Carpenter and Lodge 1986; Burkholder and Wetzel 1990). The complex nature of these direct and indirect interactions among different groups of primary producers in lake littoral zones suggest that they may be particularly sensitive to invasion by macrophytes like IWM.

IWM invasion in littoral zones may alter the biomass and production of other primary producers either by altering competition for light and nutrients, or by creating a novel growth substratum for attached algae. IWM invasion can change the physical structure of macrophyte assemblages through altering abundances of native macrophyte species. IWM is not unusually productive for an invasive species, yet it can grow fast and earlier than other macrophytes (Smith and Barko 1990). IWM has a finely dissected leaf structure on elongated stems near the water surface that have a high surface area to biomass ratio relative to other macrophyte species (Sher-Kaul et al. 1995), which may provide additional habitat for epiphytes. Mesocosm studies have found epiphytes to grow at

variable densities on macrophyte surfaces among a group of native and non-native macrophyte species, and low densities on fast growing macrophyte segments (Grutters et al. 2017). Therefore, species composition and structure of the macrophyte assemblage can impact the amount of epiphytes in the littoral zone. Canopy forming macrophytes decrease the production of epiphytes and other primary producers like benthic periphyton at the bottom of the water column (Lassen et al. 1997; Vis et al. 2006). Therefore, IWM presence may lead to shading of phytoplankton and benthic periphyton growing under IWM canopies, but offer epiphytes growing attached to IWM canopies better access to light high in the water column. We predict that presence of IWM will increase macrophyte standing crop and the available substratum for epiphytes. Because macrophytes and epiphytes can disproportionately contribute to whole-lake primary production, we further predict that areas with IWM will have higher rates of littoral zone primary production, even if shading by IWM decreases production or standing crops of phytoplankton or benthic periphyton.

The aim of this study was to determine if presence of IWM in littoral zones alters standing crops and rates of primary production by all primary producers. To address this question, we conducted a comparative study between plots where IWM was present or absent in littoral zones of 6 north-temperate lakes in Michigan and measured the standing crops of primary producers, their production rates using bottle incubations, and whole-plot production rates using open water metabolism. We then applied a mass balance approach to determine each primary producer's contribution to whole-plot primary produc-

tion. This study was designed to test the following hypotheses: 1) macrophyte and epiphyte standing crops will be higher in plots where IWM is present vs. those where it is absent due to higher biomass and vertical structure of IWM, 2) whole-plot gross primary production and ecosystem respiration rates will be higher in plots where IWM is present vs. those where it is absent due to higher standing crops or production of macrophytes and epiphytes, and 3) macrophytes and epiphytes will make larger contributions whole-plot gross primary production in plots where IWM is present vs. those where it is absent.

1.2 Methods

1.2.1 Study area

This field study was conducted July – September 2017 in littoral zones of 6 lakes in the Upper Peninsula and northern Lower Peninsula of Michigan. Waterbodies with IWM were selected based on personal observation and Michigan Invasive Species Investigation Network (MISIN) database records (Michigan State University 2018). Selected waterbodies were oligotrophic to mesotrophic and ranged in size from small inland lakes to connected waterways of the Laurentian Great Lakes (Table 1.1). Torch Lake (TCH) was the largest and deepest lake sampled (area = 11.0 km^2, mean depth 15 m), and is connected to the Keweenaw Waterway, which is connected to Lake Superior on the Keweenaw Peninsula of the Upper Peninsula. Sturgeon sloughs of Portage Lake (SLG) is a littoral habitat (area = 1.0 km^2, mean depth 2 m) also on the Keweenaw Waterway. Iron Lake (IRL) is an inland lake, 10 times smaller than Torch Lake (area = 1.6 km^2, mean depth 6 m), located in southwest Upper Peninsula. Islington Bay of Lake Huron (LCI) is

an oligotrophic, shallow enclosed bay (area = 1.6 km^2, mean depth 2 m) in the Les Cheneaux Islands region of northern Lake Huron. Horseshoe Lake (HSL) is oligotrophic and the smallest lake included in this study (area = 0.15 km^2, mean depth 3 m), located in central Lower Peninsula. Lake St. Helen (STHL) is a large lake (area = 9.7 km^2, mean depth 2 m) in central Lower Peninsula with a high percentage of littoral habitat. A paired plot design was used within each waterbody to investigate our hypothesized effects of IWM presence on littoral zone primary producers. Circular 500 m^2 plots were located in invaded (INV) macrophyte stands based on visual presence of IWM, while uninvaded (UNINV) plots were placed in nearby areas with similar macrophyte stand structure that lacked visual presence of IWM. When determining plot locations, visual observations indicated IWM stems crowded the upper water column in invaded plots of IRL, LCI, and TCH. Invaded plots in HSL, SLG, and STHL had sparser IWM stem densities and/or less occupied space, with other macrophytes also observed intermixed in the upper water column.

To describe the physical and chemical properties on each sampling date, we used a YSI 6920 sonde (YSI Incorporated, Yellow Springs, Ohio) to measure vertical profiles of temperature (°C), conductivity (mS cm^{-1}), optical dissolved oxygen (ODO) saturation (%), and ODO concentration (mg L^{-1}). Light extinction was determined from vertical profiles of light intensity collected with a Li-Cor LI193SA spherical underwater quantum sensor with a LI-1400 datalogger (LI-COR, Inc, Lincoln, Nebraska). A horizontal water sampler at 0.5 m depth was used to collect water for analysis of soluble reactive phosphorus (SRP), nitrate+nitrite (NO_3^-+NO_2^-), ammonium (NH_4^+), total dissolved nitrogen

(TDN), and dissolved organic carbon (DOC). Water was immediately filtered using Millipore 0.45 μm nitrocellulose membrane filters into 60 mL bottles and placed on ice until frozen for storage in the laboratory. SRP was analyzed on a SEAL AQ2 discrete analyzer (SEAL Analytical, Mequon, Wisconsin) based on USEPA method 365.1 revision 2.0 (USEPA 1993a) and APHA method 4500- P F (APHA 2005). NO_3^-+NO_2^- was analyzed on a SEAL AQ2 discrete analyzer (SEAL Analytical, Mequon, Wisconsin) based on USEPA method 353.2 revision 2.0 (USEPA 1993b) and APHA method 4500 NO_3^- (APHA 2005). NH_4^+ was analyzed using a fluorometric method (Holmes et al. 1999; Taylor et al. 2007) on a Turner Aquafluor (Turner Designs, Palo Alto California). TDN and DOC samples were acidified with hydrochloric acid and quantified using a Shimadzu TOC-VCSN (Shimadzu Scientific Instruments, Columbia, Maryland) (Appendix A).

1.2.2 Collection of primary producers

At each plot, aboveground macrophyte biomass was collected using fixed area sampling techniques. A 16.5 cm diameter double sided rake was lowered vertically to the lake bottom (Johnson and Newman 2011) and spun 1 revolution to collect a 0.214 m^2 sample of macrophytes; 20 of these samples were collected in a grid pattern across each plot to characterize plot-level standing crops. At 3-5 locations within each plot we collected phytoplankton, epiphytes and benthic periphyton for production and biomass analyses. Phytoplankton were collected using a horizontal water sampler lowered to 0.5 m below the surface. Epiphytes were sampled from macrophytes growing 0.5 – 1 m below the

water surface, typically *M. spicatum*, *Vallsneria americana*, or *Potomogeton* spp. Epiphytes were collected by cutting the macrophyte stem with a razor blade and allowing it to float to the water surface. The stem was carefully lifted out of the water and placed into a 2 L container with 1.8 L of lake water and agitated side to side 40 times, inverting with each direction change (Marcarelli and Wurtsbaugh 2009). This method removed loose epiphytes that were not tightly attached to macrophytes and created an epiphyte slurry. The collected macrophyte from the 2L container was removed and saved for standing crop determination as described below. Benthic periphyton was collected using a PVC sediment corer (5 cm diameter) based on a design from Gardner et al. (2009) or an Eckman grab sampler (Wetzel and Likens 2000). If the benthic material was sediment, a modified 50 mL syringe with 2.6 cm diameter open end was pushed into the sample to extract a subsample of the top 2 cm of benthic material. If the benthic material was organic flocculent, a 50 mL syringe was used to remove the top 2 cm of the whole core collected by the PVC sediment corer. Syringes of organic flocculent material were diluted by a factor of 3 before use in bottle production estimates and standing crop determination.

Sampling areas were determined for each primary producer to permit later scaling of production and standing crop measurements to the areal (whole-plot area) rates. The area of rake collections (m^2) was the sampling area for macrophytes. Epiphyte sampling area (m^2) was determined by dividing the dry mass (g) of collected macrophyte segments by the total macrophyte standing crop of each plot (g m^{-2}), determined as described below. Area of phytoplankton samples were scaled by dividing the sample volume (m^3) by

the depth of the sampling location (m) to convert to surface area (m^2). Area of benthic periphyton samples was the surface area of sample extracted by syringes from lake bottom collections (5.31 cm^2 for cores and Eckman grab samples, and 6.54 cm^2 for organic flocculent material).

1.2.3 Bottle production estimates

Production estimates for phytoplankton, epiphytes, and benthic periphyton were performed by placing collected primary producers suspended in lake water into 300 mL BOD (biological oxygen demand) bottles and sealing without any air bubbles. For each primary producer group, 3 initial bottles were filled along with 3 to 5 pairs of light and dark bottles. Dark bottles were tightly wrapped in heavy duty aluminum foil. Initial bottles were sampled at the start of the incubation period, while light and dark bottles were suspended for in situ incubation from a bar at sample collection depth (0.5 m for phytoplankton and 0.5 m for epiphytes) (Vollenweider et al. 1969; Wetzel and Likens 2000). On hard lake bottoms, a bar of benthic periphyton bottles were set on the bottom, whereas on soft lake bottoms, bottles were suspended 0.1m above the bottom to prevent immersion in the benthos. To account for production of phytoplankton in the water used to suspend benthic periphyton in BOD bottles, we collected a second set of phytoplankton samples, hereafter referred to as blanks, which were deployed at the bottom depth with the benthic periphyton bottles. Incubation durations were based on pre-study trials to determine the optimal length that would allow detection of change in dissolved oxygen while avoiding large changes in internal bottle conditions. Based on the results of these

trials, bottles with phytoplankton and blanks were incubated for 6-9 hours, while bottles with epiphytes and benthic periphyton were incubated for 2-4 hours.

To measure dissolved gas concentrations in the BOD bottles (all initials, samples, and blanks), triplicate water samples were collected by siphoning into 12 mL Exetainers (Labco, Lampeter, Wales, UK) and preserving with zinc chloride (0.67 g/L final concentration). Oxygen to Argon ratios (O_2:Ar) from each Exetainer were determined using membrane inlet mass spectrometry (MIMS) (Kana et al. 1994), and triplicates were averaged to calculate mean O_2:Ar per bottle. For each primary producer, net primary production (NPP) was determined for each light bottle and respiration (R) for each dark bottle. NPP (Eq.1) and R (Eq.2) rates (mg O_2 m^{-2} h^{-1}) were calculated as the change in O_2:Ar ratios from the average O_2:Ar of all initial bottles using the equations below. Argon saturation (Ar_{sat}) was calculated from Hamme and Emerson (2004) using the water temperature and barometric pressure at the time of sample collection into Exetainers.

$$\text{Eq. 1} \quad \text{NPP} = \frac{\left[\left(\mathrm{O_2{:}\,Ar}_{light}\right) - \left(\mathrm{O_2{:}\,Ar}_{initial}\right)\right] * \mathrm{Ar}_{sat} * \text{BOD water volume}}{\text{sampling area} * \text{duration of incubation}}$$

$$\text{Eq. 2} \quad \text{R} = \frac{\left[\left(\mathrm{O_2{:}\,Ar}_{initial}\right) - \left(\mathrm{O_2{:}\,Ar}_{dark}\right)\right] * \mathrm{Ar}_{sat} * \text{BOD water volume}}{\text{sampling area} * \text{duration of incubation}}$$

For each primary producer, GPP was calculated as mean NPP subtracted from the mean R. Benthic periphyton GPP rates were adjusted for phytoplankton in lake water by subtracting blank GPP rates, while epiphyte GPP rates were adjusted by subtracting phytoplankton GPP rates. Standard error of GPP rates calculated from NPP, R, and adjusted

for blanks was propagated as $SE_{A\pm B} = (SE^2_A + SE^2_B)^{1/2}$ (Taylor 1982; Carignan et al. 1998). After calculations, any negative GPP rates were assumed to be due to bottle effects or method error and set to zero. Adjustments of GPP to zeros was done for benthic periphyton at IRL-INV (-32.6 ± 30.7 mg O_2 m^{-2} h^{-1}), LCI-INV (-12.4 ± 35.8 mg O_2 m^{-2} h^{-1}), and STHL-INV (-27.2 ± 68.9 mg O_2 m^{-2} h^{-1}), in addition to phytoplankton at SLG-UNINV (-4.9 ± 32.5 mg O_2 m^{-2} h^{-1}).

1.2.4 Primary producer standing crop measurement

Macrophytes from twist rake samples were separated and identified to species using Fasset (1957) and Skawinski (2014), then dried at 60°C for 48 hours to constant mass to determine dry weight. Species of *Chara* and *Drepanocladus* were indistinguishable in the field and/or very difficult to physically separate and were grouped by genera. *M. spicatum* and *M. spicatum* x *sibiricum* were grouped as IWM as stated previously. Macrophyte standing crops (g m^{-2}) were determined as the means of dry weights across the sampling area of twist rake samples in each plot. The dominance of IWM at all plots was calculated using two metrics. IWM standing crops were relativized to the total standing crop of each plot (abundance of IWM in each plot %) and IWM standing crop was standardized to the maximum standing crop measured in the dataset (standardized abundance of IWM %). Macrophyte segments from epiphyte collection were identified to species and dried to constant mass and weighed.

To determine standing crops of epiphytes, phytoplankton and benthic periphyton, subsamples from each BOD bottle used for the production estimates were filtered onto

pre-ashed GF/F filters (0.7 μm). Filters were frozen until laboratory analysis of chlorophyll *a* (Chla) using ethyl alcohol extraction followed by spectrophotometric analysis with correction for phaeophytin using a Thermo Scientific 10 s UV–Vis spectrophotometer (APHA 2005). After Chla analysis, filters were analyzed for ash free dry mass (AFDM, g m^{-2}), which provides an estimate of the total organic material in a sample and is measured as the difference between the mass of the oxidized samples and the initial dry samples. AFDM samples were dried at 100 °C, weighed for dry mass and then oxidized in a muffle furnace at 550 °C, rewetted, and dried before final weighing. All masses of Chla and AFDM were divided by the sampling areas of the primary producer to calculate standing crops.

1.2.5 Open water metabolism

At the center of each plot, we deployed a YSI 6920 sonde or MiniDOT logger (PME, Vista, California) in conjunction with surface mounted Hobo light and temperature pendant loggers (Onset, Bourne, Massachusetts) for 3-9 days spanning the day(s) of primary producer bottle production and standing crop sampling. All sensors were programmed to log dissolved oxygen, temperature, and light at 10-minute intervals. A modified one-station metabolism model for multiple observation days was used to estimate GPP, ER, and air–water gas exchange using the following equation (Eq. 3, originally from Van de Bogert et al. 2007; Hotchkiss and Hall 2015).

$$\text{Eq. 3} \quad O_{2,(t)} = O_{2,(t-1)} + \left(\frac{GPP}{z} \times \frac{L_{(t-1)}}{\sum L_{24hr}}\right) + \frac{ER \times \Delta t}{z} + K_{O_2} \times \Delta t \times \left(O_{2sat,(t-1)} - O_{2,(t-1)}\right)$$

In this equation, GPP and ER are positive and negative rates of O_2 production, respectively (g O_2 m^{-2} d^{-1}), L is irradiance (lux), K_{O2} is temperature-corrected O_2 gas exchange rate (d^{-1}), and O_{2sat} is O_2 saturation concentration (g O_2 m^{-3}), and the depth at the location of sensor deployment is z. Posterior probability distributions of GPP, ER and K were simulated using Bayesian parameter estimation with uninformative priors via a random walk Metropolis algorithm and Markov chain Monte Carlo using RSTAN 2.17.3 (Stan Development Team 2018) in R version 3.4.4 (R Core Team 2018). Initially, the model was set to integrate across all measurement days to provide more robust estimates of K integrating day-to-date variability in environmental conditions (Appling et al. 2018). Yet, when there is wide variation in weather conditions among sampling dates and/or when physical parameters override biological signals (Winslow et al. 2016), these models can produce poor fits or unrealistic estimates of K, GPP or ER. Therefore, multi-day model outputs were screened for fit and ecologically unrealistic values (negative GPP or positive ER. First, days with no or poor model fit were removed (2 days IRL-UNINV, 1 day TCH-INV, 3 days TCH-UNINV). All days with ecologically un-realistic values yet good model fits (1 day SLG-UNINV, 2 days HSL-UNINV, 1 day HSL-INV) were analyzed with single day metabolism models that estimated GPP, ER and K from 24-hour periods repeated for all days with complete records. Following daily models all ecologically un-realistic values remained, so those dates were removed from analyses. Net ecosystem production (NEP) of plots was calculated at the sum of GPP and ER.

1.2.6 Production mass balance estimates

The components of GPP attributed to different primary producers (phytoplankton, epiphytes, benthic periphyton) were calculated as the daily GPP of each primary producer group divided by the average daily GPP of the plot. HSL-UNINV and IRL-UNINV did not have multiple days of metabolism results to average plot GPP, therefore only one day of plot GPP was used instead. Hourly GPP rates (mg O_2 m^{-2} h^{-1}) of primary producers were converted to daily GPP rates (g O_2 m^{-2} d^{-1}) by multiplying by the length of the daily photoperiod retrieved from NOAA's solar calculator (NOAA 2018). The portion of plot GPP by macrophytes was estimated as the remainder of plot GPP after subtracting the portions due to phytoplankton, epiphytes, and benthic periphyton. When the sum of portions of phytoplankton, epiphytes, and benthic periphyton exceeded the daily plot GPP, the sum of portions was then used as plot GPP. This occurred in HSL-INV and IRL-UNINV plots and the component of GPP due to macrophytes in these plots was set to zero.

1.2.7 Statistical analyses

To assess the integrity of our paired plot selection, plot and water characteristics along with IWM and native macrophyte standing crops were compared using two-sided paired t-tests in R 3.4.4 (R Core Team 2018). To describe the species structure of the macrophyte assemblages across lakes and study plots we used Non-metric Multidimensional Scaling (NMS) in PC-ORD v6.30 (McCune and Mefford 2011). A NMS ordination was resolved using "slow and thorough" defaults, which uses Sorensen distance measures, random starting position, 250 runs of real data, and 250 runs with randomized

data through six to one-dimensional solutions. The main matrix was 12 sites x 25 species (Appendix B); to achieve a stable ordination solution it was logarithmically transformed to reduce extreme left skewedness of distribution of standing crops while still preserving the original orders of magnitudes (McCune and Grace 2002). After transformation, rare species that were present only once in the matrix were removed, resulting in a transformed matrix of 12 sites x 15 species (Appendix C). Rare species were removed as they can have disproportionate effects on multivariate analyses and contribute little to understanding general community relationships (Jackson and Harvey 1989). Summary statistics on the main matrix were calculated using PC-ORD for species richness and evenness, Shannon's diversity, and Simpson's diversity index (Appendix D).

Comparisons of invaded and uninvaded plots were performed using paired t-tests in R 3.4.4 (R Core Team 2018). When testing hypotheses that macrophyte and epiphyte standing crops will be higher in invaded plots vs. uninvaded plots, plot GPP and ER rates will be higher in invaded vs. uninvaded plots, and macrophytes and epiphytes will be greater components of plot GPP in invaded vs. uninvaded plots, we used one-sided paired t-tests with the significance level set at alpha = 0.05. All other paired comparisons for differences between paired invaded vs. uninvaded plots were performed using two-sided paired t-tests.

Stepwise multiple linear regression performed in R 3.4.4 (R Core Team 2018) was used to identify significant predictors of phytoplankton, epiphyte, and benthic periphyton

standing crops and primary production, as well as plot GPP and ER rates. Predictors initially included were light extinction, water temperature, conductivity, TDN, DOC, NH_4^+, SRP, NO_3^-+NO_2^-, and macrophyte standing crop. Additionally, phytoplankton Chla, epiphyte Chla, and benthic periphyton Chla were included as predictors of plot GPP. Phytoplankton AFDM, epiphyte AFDM, and benthic periphyton AFDM were included as predictors of plot ER. All variables were examined for normality and homoscedasticity; when needed variables were transformed to meet the assumptions of multiple linear regression, or variables were removed if a suitable transformation was not possible. As a result, NO_3^-+NO_2^- , NH_4+, benthic periphyton Chla, epiphyte Chla, phytoplankton Chla, and benthic periphyton AFDM were logarithmically transformed for analyses. SRP was removed due to a right skewed distribution. Prior to performing regression analysis, we conducted Pearson correlation analysis to identify significant correlations ($p \leq 0.05$) among the predictor variables for each analysis (see Appendix E). For all stepwise multiple linear regression analyses, conductivity, DOC, NO_3^-+NO_2^-, and NH_4^+ were removed due to significant correlations with other predictor variables (Appendix E). For stepwise multiple linear regression analysis of plot GPP, benthic periphyton Chla was removed due to correlation with macrophyte standing crop and phytoplankton Chla was removed due to correlation with TDN (Appendix E). Additionally, for stepwise multiple linear regression analysis of plot ER, epiphyte AFDM was removed due to correlation with phytoplankton AFDM and benthic periphyton AFDM was removed due to correlation with macrophyte standing crop (Appendix E). We identified the best regression model based on the smallest Akaike's information criteria (AIC, Burnham and Anderson 2002).

1.3 Results

1.3.1 Comparison of study sites

Site and water characteristics were similar but macrophyte assemblages of plots were different between pairs of invaded and uninvaded plots. Invaded plots and uninvaded plots had similar depths (2.1 m ± 0.2 vs. 1.8 m ± 0.2, paired t-test, $t = 2.05$, $df = 5$, $p = 0.10$; Table 1.1). Water characteristics, nutrients, and light extinction were not significantly different between invaded vs. uninvaded plots (Table 1.2, Appendix A). IWM standing crop was 50-fold higher (paired t-test, $t = 3.69$, $df = 5$, $p = 0.007$) and total native macrophyte standing crop was 1-fold lower in invaded vs. uninvaded plots (paired t-test, $t = -2.20$, $df = 5$, $p = 0.04$; Figure 1.2). IWM composed 61% of the macrophyte biomass in invaded plots and 2% of the macrophyte biomass in uninvaded plots (Table 1.3). The standardized abundance of IWM in invaded plots was 31 % (Table 1.3). Species richness, species evenness, Shannon's diversity, and Simpson's diversity index was similar between invaded and uninvaded plots (Table 1.2, Appendix D). The NMS analysis of macrophyte assemblage produced an ordination from 87 iterations resolving a four-dimensional solution, stress of 1.15, and final stability < 0.00001 (Figure 1.3). 84% of variance of structure was captured by 3 of the ordination axes. Differences in ordination space between invaded and uninvaded plots were generally driven by differences in abundance of native macrophyte species and IWM (Figure 1.3, Appendix F). The first axis (Axis 1) represented 57% of the variance. Macrophytes with strong positive correlation to Axis 1 were *Potamogeton robbinsii* ($r = 0.77$), *P. amplifolius* ($r = 0.72$), and IWM ($r =$

0.66). Macrophytes with a strong negative correlation with Axis 1 were *Vallisneria americana* (r = -0.83), *Najas flexilis* (r = -0.57), *P. gramineus* (r = -0.56), *Ceratophyllum demersum* (r = -0.54), and *Bidens becki* (r = -0.43). The second axis (Axis 2) represented 11% of the variance. Macrophytes with strong positive correlation to Axis 2 were *B. becki* (r = 0.52) and *P. robbinsii* (r = 0.48) and strong negative correlations were *Chara* spp. (r = -0.71), *N. guadalupensis* (r = -0.69), *P. zoosteriformis* (r = -0.67), and *N. flexilis* (r = -0.51). The third axis (Axis 3) represented 16% of the variance. Macrophytes with strong positive correlation to Axis 3 were *Elodea canadensis* (r = 0.86), *B. becki* (r = 0.61), *Utricularia macrorhiza* (r = 0.57), *P. richardsonii* (r = 0.54), *C. demersum* (r = 0.47), and IWM (r = 0.42). Macrophytes with a strong negative correlation with Axis 3 were *N. flexilis* (r = -0.49) and *P. gramineus* (r = -0.46) (Figure 1.3, Appendix F).

1.3.2 Primary production rates

GPP of primary producers was similar between invaded and uninvaded plots, but across all plots GPP for benthic periphyton and phytoplankton were higher in in warmer water. GPP rates of epiphytes, phytoplankton, and benthic periphyton were not significantly different between invaded and uninvaded plots (epiphytes paired t-test, t = 0.41, df = 5, p = 0.70; phytoplankton paired t-test, t = 1.44, df = 5, p = 0.21; benthic periphyton paired t-test, t = -1.25, df = 5, p = 0.27) (Figure 1.4). Benthic periphyton GPP rates were the most variable with high standard errors (on average 56.9 ± 56.8, SE up to 217.6 mg O_2 m^{-2} h^{-1}). Stepwise multiple linear regression identified significant models that explained about 1/2 of the variation in benthic periphyton and phytoplankton GPP (Table

1.4). Benthic periphyton GPP was negatively related to macrophyte standing crop and positively related to water temperature with $R^2_{adj} = 0.50$ and $p = 0.02$, while phytoplankton GPP was positively related to water temperature with $R^2_{adj} = 0.46$ and $p = 0.009$ (Table 1.4).

1.3.3 Standing Crops

Standing crops of primary producers were similar between invaded and uninvaded plots. Total macrophyte standing crops in study plots ranged from 16.6 - 307.7 g m^{-2} (Figure 1.2). Although we hypothesized higher total macrophyte biomass in invaded plots, the total macrophyte biomass at paired invaded vs. uninvaded plots was not significantly higher (Figure 1.2, paired t-test, $t = 0.43$, $df = 5$, $p = 0.34$). Also, epiphyte chlorophyll *a* (paired t-test, $t = -0.40$, $df = 5$, $p = 0.35$) and AFDM (paired t-test, $t = -0.53$, $df = 5$, $p = 0.31$) were not significantly higher in invaded vs. uninvaded plots (Figure 1.5). Phytoplankton Chla and AFDM was not significantly different between paired invaded vs. uninvaded plots (Chla paired t-test, $t = -0.01$, $df = 5$, $p = 0.99$; AFDM paired t-test, $t = -1.10$, $df = 5$, $p = 0.32$). Also, benthic periphyton Chla and AFDM was not significantly different between paired invaded vs. uninvaded plots (Chla paired t-test, $t = 0.36$, $df = 5$, $p = 0.73$; AFDM paired t-test, $t = 0.33$, $df = 5$, $p = 0.76$) (Figure 1.5). Benthic periphyton standing crops were generally one order of magnitude higher than phytoplankton and two orders of magnitude higher than epiphytes, as quantified by both chlorophyll *a* and

AFDM (Figure 1.5). However, it should be noted that AFDM of benthic periphyton included sediment organic matter collected in the core, and not strictly the benthic periphyton.

Stepwise multiple linear regression identified significant models for Chla and AFDM of benthic periphyton and phytoplankton. Benthic periphyton Chla was positively related to water temperature and negatively related to macrophyte standing with $R^2_{adj} = 0.49$, but benthic periphyton AFDM was positively related to macrophyte standing crop and negatively related to light extinction coefficients with $R^2_{adj} = 0.47$ (Table 1.4). Phytoplankton Chla was positively related to TDN and macrophyte standing crop with $R^2_{adj} = 0.65$, while phytoplankton AFDM was positively related to water temperature with $R^2_{adj} = 0.30$ (Table 1.4). No significant models were produced for epiphyte Chla and AFDM (Table 1.4).

1.3.4 Open water metabolism

Plot GPP and ER were similar between invaded and uninvaded plots. Plots had a wider range of ER (-2.8 to -12.5 g O_2 m^{-2} d^{-1}) than GPP rates (1.1 – 7.7 g O_2 m^{-2} d^{-1}). GPP (paired t-test, t = 0.62, df = 5, p = 0.28) and ER (paired t-test, t = 0.63, df = 5, p = 0.18) rates were not significantly higher in invaded vs. uninvaded plots (Figure 1.6). During the time of sampling, most plots were heterotrophic with a range of NEP rates from 2.6 to -11.4 g O_2 m^{-2} d^{-1}. Stepwise multiple linear regression did not identify significant models for GPP and ER rates of plots (Table 1.4). A model with $p = 0.06$ suggested that plot ER was negatively related to water temperature with $R^2_{adj} = 0.25$ (Table 1.4).

1.3.5 Production mass balance

Mass balance analysis to determine the contributions of GPP from different primary producers revealed that contributions differed among lakes based on observations of canopy development in the study plots. Macrophytes (paired t-test, $t = 1.35$, $df = 5$, $p = 0.23$) and epiphytes (paired t-test, $t = -0.78$, $df = 5$, $p = 0.76$) did not comprise significantly higher portions of plot GPP in invaded vs. uninvaded plots as we hypothesized they would (Fig. 1.7). Additionally, portions of plot GPP from phytoplankton (paired t-test, $t = -0.32$, $df = 5$, $p = 0.76$), and benthic periphyton (paired t-test, $t = -1.18$, $df = 5$, $p = 0.29$) were not significantly different between invaded and uninvaded plots. But, invaded plots in IRL, LCI, and TCH showed ca. 27% lower portions of plot GPP by benthic periphyton compared to uninvaded plots (Figure 1.7). The invaded plots in these 3 lakes had higher standard abundances of IWM (30-56%) and had dense upper water column of IWM, while the other invaded plots had lower standard abundances (7-23 %) and sparse upper water column densities of IWM (Table 1.3).

1.4 Discussion

We found that IWM had limited effects on primary producer standing crops and rates of primary production across our north-temperate study lakes. Contrary to our hypotheses that IWM presence would lead to higher macrophyte and epiphyte standing crops, higher whole-plot GPP and ER, and higher contributions of macrophytes and epiphytes to whole-plot GPP, we found that standing crops, primary production by all pri-

mary producer groups, and plot-level GPP and ER rates were not different between invaded and uninvaded plots. Stepwise multiple linear regression analysis of the variables predicting productivity and primary producer standing crop across all study plots identified macrophyte standing crop as a driver of benthic periphyton GPP and standing crops of all other primary producers, along with water temperature, nutrient concentrations, and clarity. These findings suggest that the drivers of littoral zone primary production were not different from when IWM was present or absent in our study. These findings also agree with the findings of other studies that macrophyte standing crops can be an important control on within-lake processes in whole lakes (Lauster et al. 2006; Van de Bogert et al. 2012) or on the landscape scale.

We expected to observe large differences in macrophyte and associated epiphyte standing crops between invaded and uninvaded plots, particularly because we sampled late in the summer when macrophytes tend to reach their highest biomasses. We observed that in our study plots, IWM generally grew integrated with the native macrophyte assemblage, with 1-fold lower abundances of native macrophytes. Half of the invaded plots had dense shoots of IWM in the upper water column, while the other half had sparse shoot density in the upper water column. None of our invaded plots had thick IWM canopies that can form by sprawling shoots lying flat on the water's surface. Other studies have documented reduced macrophyte diversity or complete displacement of native species when IWM form these dense canopies (Madsen et al. 1991; Boylen et al. 1999). The lack of dense surface canopies of IWM may have led to the weak effects observed in our

study. Even though macrophyte standing crops of our study plots were not different, macrophyte species can provide varying amounts of surface areas (Sher-Kaul et al. 1995) for epiphytes, which we did not quantify in our study. We sampled epiphytes from a subset of species that grew into the upper water column and incubated all epiphyte samples at a common depth, which may have homogenized estimates of epiphyte production between plots. Collecting and incubating epiphytes at the upper, mid, and lower depths of the macrophyte assemblage would have provided a more accurate estimate of epiphyte production (Vis et al. 2006).

It is also unlikely that limiting factors of nutrients or the interaction between primary producers were different between paired invaded vs. uninvaded plots in our study. Physical and water characteristics that commonly limit production rates like nutrients, lake morphology, and water clarity were not significantly different among invaded and uninvaded plots. Effects of IWM on the standing crops or production of all other littoral primary producers was not detected between the paired plots. When using stepwise multiple linear regression to analyze the production and standing crop of primary producers across all plots, macrophyte standing crop was detected as a driver of rates for benthic periphyton GPP and standing crops of all other primary producers. One likely mechanism for this effect is shading by macrophytes, but nutrient competition and other direct and indirect interactions (e.g., Figure 1.1) could also be driving these relationships. Macrophyte biomass was positively related to benthic periphyton AFDM, possibly due to macrophyte detritus accumulating in the benthos. Phytoplankton Chla was positively related to macrophyte standing crop in addition to TDN concentration, and phytoplankton GPP

had a strong positive relation to water temperature. A possible mechanism for the relationship of phytoplankton Chla with macrophytes standing crop and TDN is the sloughing of epiphytes from macrophytes, but other direct and indirect interactions (e.g., Figure 1.1) could also drive this relationship. IWM dominance of macrophyte assemblages was generally low in the north-temperate lakes in this study. The distribution of species follows a universal pattern that holds true even for invasive species; species are commonly found in low abundances in most locations and abundant in a few (Hansen et al. 2013). Surveys of invasive plants of the coastal wetlands of the Great Lakes found that Eurasian watermilfoil was present at 61% of lakeshore segments surveyed with an average plant community dominance of 19% (Trebitz and Taylor 2007). In our study, invaded plots had an average standardized abundance (dominance) of 31%. Half of our invaded plots had dense upper water column of IWM and higher than average standard abundances (30-56%). In these plots there was a pattern of decreased benthic periphyton GPP in the invaded plots relative to the uninvaded plots. Our findings may be different if our study had captured IWM that dominated macrophyte assemblages and formed dense surface canopies, but these conditions are relatively rare considering species distributions (Hansen et al. 2013). Alternatively, large effects of IWM presence on primary production may be predicted where IWM was present in an area that was previously unvegetated. For example, invasions of IWM into unvegetated areas have been reported in the Tennessee Valley Association reservoirs and Lake Opinicon, Ontario (Keast 1984; Smith and Barko 1990). Regardless in many lakes, IWM may not dominate macrophyte assemblages, and our results suggest that in these lakes IWM presence may not alter rates of primary production

in littoral zones. Instead, littoral zone productivity would continue to be governed by the factors that commonly control lake productivity across landscapes: water temperature, light availability, and nutrient supply. Therefore, invasive watermilfoil may have little impact on primary production yet macrophyte standing crops are an important direct and indirect influences on lake processes.

2 Seasonal Dynamics of Primary Production in Littoral Zones of North-Temperate Lakes

2.1 Introduction

A better understanding of seasonal ecosystem dynamics is essential to estimate and predict effects of climate change on ecological processes in north-temperate lakes. Anthropogenic climate change has increased water temperatures in aquatic systems, and lakes in the northern hemisphere have experienced decreased winter ice duration coupled with increased strength and duration of summer water temperature and stratification (De Stasio et al. 1996; Magnuson 2009). The prevailing paradigm is that ice cover and low water temperatures during winter establish an inactive period for primary producers, but studies that include under-ice measurements suggest biological processes are both active and complex, with almost no data available currently for benthic processes (Hampton et al. 2016). Most winter limnology studies that occur only sample in the middle of the open-water pelagic zones of lakes which has limited inference of primary productivity of the whole lake (Van de Bogert et al. 2012). The shallow water habitat of lakes, called littoral zones, are annually key locations of productivity in lakes (Vadeboncoeur et al. 2011) because they extend from the shore to a depth where warm summer surface waters (Horne and Goldman 1994) and sufficient light reach the lake bottom for primary producers (Dodds and Whiles 2010). A key knowledge gap in our understanding of lakes is how rates of primary production vary in littoral zones through all seasons, including winter.

The littoral zones of lakes host diverse groups of primary producers which are important to whole lake productivity. These primary producers include attached algae,

aquatic plants (macrophytes), and suspended phytoplankton. Phytoplankton are small free floating algae ranging from microscopic single cells to colonial algae the size of peas (Horne and Goldman 1994). Attached algae include diatoms, filamentous green algae, and cyanobacteria (Horne and Goldman 1994), which can be found growing on bottom substrates (benthic periphyton) and attached to macrophytes (epiphytes). Macrophytes include emergent and submerged aquatic plants, which display a diversity of growth forms and types under different conditions. Macrophytes grow vertically in the water column, providing large surface areas and morphologically determined microhabitats for epiphytes (Ferreiro et al. 2013), while also shading primary producers growing lower in the water column and on the benthos. The contributions of macrophytes to primary production are enhanced by the production of the attached epiphytes, which can be a major component of whole lake production. For example, in a small, shallow oligotrophic lake in southern Michigan, phytoplankton accounted for about 25% of annual net primary production, while attached algae contributed 22%, and macrophytes contributed 51% (Wetzel et al. 1972).

Seasonal patterns of growth and production are key for understanding the dynamics of the entire community of primary producers in these zones. In temperate climates, the overall primary production in lakes drops in autumn and into the winter, returning to peak productivity in spring and summer (Staehr and Sand-Jensen 2007). Although it is generally assumed that macrophyte production ceases seasonally due to temperature and light limitation (Scheffer 1998), ten macrophyte species maintained substantial biomass and produced 10-20% of their midsummer primary production overwinter in a New York

lake (Boylen and Sheldon 1976). In temperate lakes, most macrophytes grow from tubers, turions, or seeds once waters warm in the spring and reach peak biomasses during summer. In autumn, plants senesce and decompose as the water cools (Scheffer 1998). In contrast to the lack of study on macrophytes across all seasons, seasonal dynamics of phytoplankton in temperate, dimictic lakes are well generalized. One synthesis by the Plankton Ecology Group model (Sommer et al. 1986) shows that phytoplankton biomass is low in the winter, but blooms of diatoms occur in the spring and autumn as thermal stratification and destratification occurs. Nutrient limitation, resource competition, and predation keep phytoplankton biomass low during summer stratification (Horne and Goldman 1994). The few studies of seasonal patterns of attached algae show a significant correlation with light and water temperature, with highest primary production during mid-summer and low primary production in winter (Liboriussen and Jeppesen 2003). In Lake Memphragog (Quebec-Vermont), epiphytes on *Myriophyllum spicatum* had low primary production in the summer likely due to grazing yet displayed its highest primary production late autumn. In the same lake, epiphyte production on *Potamageton richardsonii* was minimal except during early summer (Cattaneo and Kalff 1980). Many studies have measured primary production in the pelagic zones across all seasons, or in littoral zones during the growing season. But none to our knowledge have measured production of all primary producers in littoral zones across seasons.

The aim of this project was to fill key knowledge gaps of the seasonal dynamics of littoral primary producers including winter. We conducted a field study in two lakes to measure whole-plot production rates using open water metabolism, the standing crops of

primary producers, and the production of phytoplankton, epiphytes and benthic periphyton using bottle incubations across a full year. This study was designed to test the following hypotheses: 1) gross primary production (GPP) of all littoral primary producers will be lowest during the winter and highest during the summer due to seasonal changes in water temperature and light (Figure 2.1a), 2) Macrophyte standing crops will increase late spring, peak in the summer and diminish late autumn, 3) Epiphyte standing crops will be highest in late summer and diminish in autumn coincident with decreasing macrophyte standing crops, 4) Phytoplankton standing crop will be highest in spring and autumn due to water column mixing, and 5) Benthic periphyton standing crops will increase in spring, decrease in summer due to macrophyte shading, reach highest levels in the autumn, and decrease in winter (Figure 2.1b).

2.2 Methods

2.2.1 Study area

This field study was conducted July 2017 – July 2018 in littoral zones of 2 small inland lakes in the Upper Peninsula of Michigan (Figure 2.2a). Lakes were selected based abundant littoral habitat and availability of public winter access with stabile ice conditions. Rice Lake is 2.73 km^2 in area with a maximum depth of 3 m and forested shorelines that are sparsely developed with cabins (Figure 2.2b). The littoral zone has sand substrates that switches to pulpy peat beyond the 1.5 m contour (Michigan Department of Natural Resources 2018). Thayers Lake is 0.47 km^2 in area and 3.1 m at the deepest point on one half of the lake (Figure 2.2b, Michigan Department of Natural Resources 2018).

The shallow half of the lake is 1m deep with abundant submerged macrophytes, and the substrate in most of the lake is comprised of organic materials. Thayers Lake is undeveloped and surrounded by marsh with two creek inflows and one outflow. In each lake a circular 500 m^2 study plot was established in the littoral habitat in greater than 1 m of water to allow adequate water depth for winter sampling. Plots were sampled at least once per summer (June to August), autumn (September to November), winter (December to April), and spring (May). During periods of open water, a boat was used to sample plots; during ice cover gear was hauled out on toboggans. Holes in the ice were cut with an ice auger and an ice saw to collect samples and deploy equipment.

To describe the physical and chemical properties on each sampling date, we used a YSI 6920 sonde (YSI Incorporated, Yellow Springs, Ohio) to measure vertical profiles of temperature (°C), conductivity (mS cm^{-1}), optical dissolved oxygen (ODO) saturation (%), and ODO concentration (mg L^{-1}). Light extinction was determined from vertical profiles of light intensity collected with a Li-Cor LI193SA spherical underwater quantum sensor with a LI-1400 datalogger (LI-COR, Inc, Lincoln, Nebraska) (Table 1). When ice cover was present light measurements captured light at the surface, and the vertical profiles below the ice. A horizontal water sampler at 0.5 m depth was used to collect water for analysis of soluble reactive phosphorus (SRP), nitrate+nitrite (NO_3^-+NO_2^-), ammonium (NH_4^+), total dissolved nitrogen (TDN), and dissolved organic carbon (DOC). Water was immediately filtered using Millipore 0.45 μm nitrocellulose membrane filters into 60 mL bottles and placed on ice until frozen for storage in the laboratory. SRP was analyzed on a SEAL AQ2 discrete analyzer (SEAL Analytical, Mequon, Wisconsin) based

on USEPA method 365.1 revision 2.0 (USEPA 1993a) and APHA method 4500- P F (APHA 2005). NO_3^-+NO_2^- was analyzed on a SEAL AQ2 discrete analyzer (SEAL Analytical, Mequon, Wisconsin) based on USEPA method 353.2 revision 2.0 (USEPA 1993b) and APHA method 4500 NO_3^- (APHA 2005). NH_4^+ was analyzed using a fluorometric method (Holmes et al. 1999; Taylor et al. 2007) on a Turner Aquafluor (Turner Designs, Palo Alto California). TDN and DOC samples were acidified with hydrochloric acid and quantified using a Shimadzu TOC-VCSN (Shimadzu Scientific Instruments, Columbia, Maryland)

2.2.2 Open water metabolism

At the center of each plot, we deployed a YSI 6920 sonde or MiniDOT logger (PME, Vista, California) for 3-10 full days spanning each sampling period. Sensors were programmed to log dissolved oxygen and temperature at 10-minute intervals. Photosynthetically active radiation (PAR) data recorded in 10-minute intervals needed for metabolism models was retrieved from the GLRC Waterfront Meteorological Station (Michigan Technological University et al. 2018) due to its proximity to study locations (< 28 km) and availability of year-round measurements. A modified one-station metabolism model for multiple observation days to estimate GPP, ER, and air–water gas exchange using the following equation (Eq.4, originally from Van de Bogert et al. 2007; Hotchkiss and Hall 2015).

$$Eq.4 \quad O_{2,(t)} = O_{2,(t-1)} + \left(\frac{GPP}{z} \times \frac{L_{(t-1)}}{\sum L_{24hr}}\right) + \frac{ER \times \Delta t}{z} + K_{O_2} \times \Delta t \times \left(O_{2sat,(t-1)} - O_{2,(t-1)}\right)$$

In this equation, GPP and ER are positive and negative rates of O_2 production, respectively (g O_2 m^{-2} d^{-1}), L is light data as PAR, K_{O2} is temperature-corrected O_2 gas exchange rate (d^{-1}), and O_{2sat} is O_2 saturation concentration (g O_2 m^{-3}), and the depth at the location of sensor deployment is z. When metabolism measurements were collected in spring, summer, and autumn, posterior probability distributions of GPP, ER and K were simulated using Bayesian parameter estimation with uninformative priors via a random walk Metropolis algorithm and Markov chain Monte Carlo using RSTAN 2.17.3 (STAN Development Team, 2018) in R version 3.4.4 (R Core Team, 2018). The Bayesian model was set to integrate across all measurement days to estimate K to remove the effect of day-to-date variability in environmental conditions. When metabolism measurements were collected in the winter under ice cover, we used the streamMetabolizer package version 0.10.9 (github.com/USGS-R/streamMetabolizer) in R version 3.4.4 (R Core Team, 2018) to run a Maximum Likelihood Estimation (MLE) model with K manually set to zero for all sample days to solve for GPP and ER. When there is wide variation in weather conditions among sampling dates and/or when physical parameters override biological signals (Winslow et al. 2016), these unconstrained models can product poor fits or unrealistic estimates of K, GPP or ER (Appling et al. 2018). Therefore, model outputs were screened for fit and ecologically unrealistic values (negative GPP or positive ER). Dates with ecologically un-realistic values were removed from further analysis. This applied to 38 out of combined 152 modeled days; 22 of the 38 removed dates were from winter metabolism estimates.

2.2.3 Collection of primary producers

Within each plot, aboveground macrophyte biomass was collected using fixed area sampling techniques. A 16.5 cm diameter double sided rake was lowered vertically to the lake bottom (Johnson and Newman 2011) and spun 1 revolution to collect a 0.214 m^2 sample to determine macrophyte standing crop. During periods without ice cover, 20 samples were collected in a grid pattern across each plot to characterize plot-level standing crops. During winter, this was reduced to 10-12 samples collected through augured holes in the ice in a grid pattern. At 3-5 locations within each plot we collected phytoplankton, epiphytes and benthic periphyton for production and biomass analyses. Phytoplankton were collected using a horizontal water sampler lowered to 0.5m depth. Epiphytes were collected by cutting a macrophyte stem with a razor blade and allowing it to float to the water surface. The stem was carefully lifted out of the water and placed into a 2 L container with 1.8 L of lake water and agitated side to side 40 times, inverting with each direction change (Marcarelli and Wurtsbaugh 2009). This method removed loose epiphytes that were not tightly attached to macrophytes and created an epiphyte slurry. The collected macrophyte from the 2L container was removed and saved for standing crop determination as described below. Epiphytes were not collected in winter as macrophytes stems were laying low to the lake bottom and could not be collected in a way that would prevent separation of epiphytes during collection. Benthic periphyton was collected using a PVC sediment corer (5 cm diameter) based on a design from Gardner et al. (2009) or an Eckman grab sampler (Wetzel and Likens 2000). If the benthic material was sedi-

ment, a modified 50 mL syringe with 2.6 cm diameter open end was pushed into the sample to extract a subsample of the top 2 cm of benthic material. If the benthic material was organic flocculent, a 50 mL syringe was used to remove the top 2 cm of the whole core collected by the PVC sediment corer. Syringes of organic flocculent material were diluted by a factor of 3 before use in bottle production estimates and standing crop determination.

Sampling areas were determined for each primary producer to permit later scaling of production and standing crop measurements to the areal (whole-plot area) rates. The area of rake collections (m^2) was the sampling area for macrophytes. Epiphyte sampling area (m^2) was determined by dividing the dry mass (g) of collected macrophyte segments by the total macrophyte standing crop of each plot (g m^{-2}), as described below. Area of phytoplankton samples were scaled by dividing the sample volume (m^3) by the depth of the sampling location (m) to convert to surface area (m^2). Area of benthic periphyton samples was the surface area of sample extracted by syringes from lake bottom collections (5.31 cm^2 for cores and Eckman grab samples, and 6.54 cm^2 for organic flocculent material).

2.2.4 Bottle production estimates

Production estimates for phytoplankton, epiphytes, and benthic periphyton were performed by placing primary producers suspended in lake water into 300 mL BOD (biological oxygen demand) bottles and sealing without any air bubbles. For each primary

producer group, 3 initial bottles were filled along with 3 to 5 pairs of light and dark bottles. Dark bottles were tightly wrapped in heavy duty aluminum foil. Initial bottles were sampled at the start of the incubation period, while light and dark bottles were suspended for in situ incubation from a bar at sample collection depth (0.5 m for phytoplankton and 0.5 m for epiphytes) (Vollenweider et al. 1969; Wetzel and Likens 2000). On hard lake bottoms, a bar of benthic periphyton bottles were set on the bottom, whereas on soft lake bottoms, bottles were suspended 0.1m above the bottom to prevent immersion in the benthos. To account for production of phytoplankton in the water used to suspend benthic periphyton in BOD bottles, we collected a second set of phytoplankton samples, hereafter referred to as blanks, which were deployed at the bottom depth with the benthic periphyton bottles. Incubation durations were based on pre-study trials to determine the optimal length that would allow detection of change in dissolved oxygen while avoiding large changes in internal bottle conditions. Based on the results of these trials, bottles with phytoplankton and blanks were incubated for 6-9 hours, while bottles with epiphytes and benthic periphyton were incubated for 2-4 hours.

To measure dissolved gas concentrations in the BOD bottles (all initials, samples, and blanks), triplicate water samples were collected by siphoning into 12 mL Exetainers (Labco, Lampeter, Wales, UK) and preserving with zinc chloride (0.67 g/L final concentration). Oxygen to Argon ratios (O_2:Ar) from each Exetainer was determined using membrane inlet mass spectrometry (MIMS) (Kana et al. 1994), and triplicates were averaged to calculate mean O_2:Ar per bottle. For each primary producer, net primary production (NPP) was determined for each light bottle and respiration (R) for each dark bottle.

NPP (Eq.5) and R (Eq.6) rates (mg O_2 h^{-1}) were calculated as the change in O_2:Ar ratios from the average O_2:Ar of all initial bottles. Argon saturation (Ar_{sat}) was calculated from Hamme and Emerson (2004) using the water temperature and barometric pressure at the time of sample collection into Exetainers.

$$\text{Eq. 5} \quad \text{NPP} = \frac{\left[\left(\mathrm{O_2{:}\,Ar}_{light}\right) - \left(\mathrm{O_2{:}\,Ar}_{initial}\right)\right] * \mathrm{Ar}_{sat} * \text{BOD water volume}}{\text{duration of incubation}}$$

$$\text{Eq. 6} \quad \text{R} = \frac{\left[\left(\mathrm{O_2{:}\,Ar}_{initial}\right) - \left(\mathrm{O_2{:}\,Ar}_{dark}\right)\right] * \mathrm{Ar}_{sat} * \text{BOD water volume}}{\text{duration of incubation}}$$

For each primary producer, GPP was calculated as mean NPP subtracted from the mean R. Benthic periphyton GPP rates were adjusted for phytoplankton in lake water by subtracting blank GPP rates, while epiphyte GPP rates were adjusted by subtracting phytoplankton GPP rates. At each calculation step, addition and subtraction errors in calculating GPP rates from NPP, R, or adjusting primary producer GPP rate was accounted for by propagating standard error (SE) as $SE_{A\pm B} = (SE^2_A + SE^2_B)^{1/2}$ (Taylor 1982; Carignan et al. 1998). Hourly GPP rates (mg O_2 h^{-1}) of primary producers were converted to daily GPP rates (g O_2 d^{-1}) by multiplying hourly rates by the length of the daily photoperiod retrieved from NOAA solar calculator (NOAA 2018). After calculations, any negative GPP rates were assumed to be due to bottle effects or method error and set to zero while keeping measured SE. This occurred most often with phytoplankton GPP affecting rate estimated on 3 dates in both lakes. This also affected rates estimated on 2 dates for benthic periphyton in both lakes and 1 date for epiphytes in Rice Lake. GPP was scaled relative to plot area by dividing by sampling areas determined for each primary producer. GPP

rates of benthic periphyton had variable means with high error rates and not included for further analysis. This also prevented us from using a mass balance approach to estimate macrophyte GPP, as was explained and completed in Chapter 1.

2.2.5 Primary producer standing crop measurements

Macrophytes from twist rake samples were separated and identified to species using Fasset (1957) and Skawinski (2014), then dried at 60°C for 48 hours to constant mass to determine dry weight. Species of *Chara* and *Drepanocladus* were indistinguishable in the field and/or very difficult to physically separate and were grouped as genera. We also encountered a substantial standing crop of a freshwater sponge species (possibly *Spongilla lacustris* based on descriptions in Jewell (1935)) which we included with macrophytes, recorded as genus *Spongilla*. Macrophyte standing crops (g m^{-2}) were determined as the means of dry weights across twist rake samples in each plot. Macrophyte segments from epiphyte collection were identified to species and dried to constant mass and weighed.

To determine standing crops of epiphytes, phytoplankton and benthic periphyton, subsamples from each BOD bottle used for the production estimates were filtered onto pre-ashed GF/F filters (0.7 μm). Filters were frozen until laboratory analysis of chlorophyll *a* (Chla) using ethyl alcohol extraction followed by spectrophotometric analysis with correction for phaeophytin using a Thermo Scientific 10 s UV–Vis spectrophotometer (APHA 2005). After Chla analysis, filters were analyzed for ash free dry mass (AFDM, g m^{-2}), which provides an estimate of the total organic material in a sample and

is measured as the difference between the mass of the oxidized samples and the initial dry samples. AFDM samples were dried at 100 °C, weighed for dry mass and then oxidized in a muffle furnace at 550 °C, rewetted, and dried before a final weighing. All masses of Chla and AFDM were divided by the sampling areas of the primary producer to calculate standing crops.

2.2.6 Statistical Analyses

To describe the species structure of the macrophyte assemblages through the study period we used Non-metric Multidimensional Scaling (NMS) in PC-ORD v7.07 (McCune and Mefford 2018). A NMS ordination was resolved using "slow and thorough" defaults, which uses Sorensen distance measures, random starting position, 250 runs of real data, and 250 runs with randomized data through six- to one-dimensional solutions. The main matrix was 13 plots x 21 species (Appendix G). Summary statistics of main matrix of species richness and evenness, Shannon's diversity, and Simpson's diversity index was calculated using PC-ORD (Appendix H).

Seasonal trends in individual lakes were graphically analyzed and descriptive statistics calculated to assess the hypotheses outlined above. To evaluate whether production was linked to seasonal changes in water temperature and light availability, simple linear regressions were performed in R 3.4.4 (R Core Team, 2018) using data from both lakes combined. In addition, we evaluated whether standing crops of epiphytes and benthic periphyton were linked to macrophyte standing crops using simple linear regressions. Variables of primary producer standing crops, primary producer GPP, water temperature, and

the % light at 1m depth were assessed for normality and logarithmically transformed when needed to meet the assumption of homoscedasticity for regression analysis. As a result, epiphyte Chla, epiphyte AFDM, benthic periphyton Chla, and macrophyte standing crops were all logarithmically transformed.

To evaluate other possible environmental factors that could be related to rates of productivity that were not explicitly mentioned in the hypotheses, we performed stepwise multiple linear regressions to identify significant predictors of production and standing crops of all primary producers. Predictors initially included were percent light at 1m depth, light extinction, water temperature, macrophyte standing crop, conductivity, NH_4^+, SRP, and NO_3^-+NO_2^-. Additionally, phytoplankton Chla and benthic periphyton Chla were included as predictors of plot GPP. Phytoplankton AFDM and benthic periphyton AFDM were included as predictors of plot ER. Epiphyte AFDM and Chla was not included as predictors of plot GPP or ER due to the limited data. All variables were examined for normality and homoscedasticity and then transformations attempted to meet these assumptions of multiple linear regression, or variables were removed. As a result, conductivity, NH_4^+, macrophyte standing crop, phytoplankton Chla, epiphyte Chla, benthic periphyton Chla, phytoplankton AFDM, epiphyte AFDM, and plot ER were all logarithmically transformed. SRP and NO_3^-+NO_2^- were removed due to non-normality that could not be corrected with transformation. Prior to performing regression analysis, we conducted Pearson correlation analysis to identify significant correlations ($p \leq 0.05$) among the predictor variables for each analysis (see Appendix I). For all stepwise multi-

ple linear regression analyses, percent light at 1 m depth, conductivity, and NH_4^+ were removed due to significant correlations with other predictor variables (Appendix I). For stepwise multiple linear regression analysis of plot GPP, phytoplankton Chla and benthic periphyton Chla was removed due to correlations with other predictors (Appendix I). Additionally, for stepwise multiple linear regression analysis of plot ER, periphyton AFDM was removed due to correlation with benthic periphyton AFDM (Appendix I). Before each stepwise multiple linear regression analysis, a matrix of selected predictor variables and response variable was created, then rows with missing values in the matrix were removed. We identified the best regression model based on the smallest Akaike's information criteria (AIC, Burnham and Anderson 2002).

2.3 Results

2.3.1 Site Characteristics

Water levels fluctuated by 0.3m in both lakes across seasons. Ice depth was 0.75m on Thayers Lake at the end of winter and 0.5-0.6 m on Rice Lake (Table 2.1). Water temperature, percent DO saturation, and the percent of surface irradiance at 1m water depth all had the lowest values in the winter during ice-cover (Figure 2.3). Dissolved oxygen levels were hypoxic in littoral habitats at the end of winter ranging from 1.25-3.88 mg/L. In Thayers Lake, conductivity increased 12-fold, NH_4^+ increased 13-fold, NO_3^-+NO_2^- increased 8-fold, and SRP increased 1-fold during the winter compared to the other dates (Table 2.1). In Rice Lake during the summer and winter NH_4^+ was 3-fold higher, NO_3^-

$+NO_2^-$ was 5-fold higher, and SRP was 3-fold higher compared to spring and autumn (Table 2.1).

2.3.2 Standing Crops

The species structure of macrophyte assemblages was different between Rice and Thayers Lake. The most common macrophyte species in Rice Lake in order were *Potamogeton amplifolius*, *Myriophyllum humile, Chara* spp., *Elocharis robinsii*, and *Bidens becki*. The most common macrophyte species in Thayers Lake in order were *Chara* spp., aquatic moss spp., *Vallisneria americana*, *M. heterophyllum*, and *Utricularia purpurea*. The NMS analysis of macrophyte assemblages produced an ordination from 89 iterations resolving a two-dimensional solution, stress of 5.87, and final stability < 0.00001 (Fig. 2.4). 91% of variance of structure was captured the ordination axes. The first axis (Axis 1) represented 79% of the variance. Macrophytes with strong positive correlation to Axis 1 were aquatic moss spp. (r = 0.71), *M. sibiricum* (r = 0.61), *U. intermedia* (r = 0.49), and *U. macrorhiza* (r = 0.42). Macrophytes with a strong negative correlation with Axis 1 were *M. humile* (r = -0.71), *P. amplifolius* (r = -0.67), *Chara* spp. (r = -0.50), *Elocharis robbinsii* (r = -0.49), and *Bidens becki* (r = -0.43) (Figure 2.4; Appendix J). The second axis (Axis 2) represented 12% of the variance. Macrophytes with strong positive correlation to Axis 2 were *U. intermedia* (r = 0.53), *Elocharis robbinsii* (r = 0.53), *P. amplifolious* (r = 0.48), *Bidens becki* (r = 0.45), and *Spongilla* spp. (0.42). Macrophytes with a strong negative correlation with Axis 2 were *Vallisneria americana* (r = -0.68), *Najas flexis* (r = -0.63), *M. heterophyllum* (r = -0.50), and *U. pupurea* (r = -0.50) (Appendix J).

Standing crops and the species structure of macrophyte assemblages in Rice and Thayers Lake changed seasonally. Winter macrophyte standing crops were 14% and 33% of the maximum standing crops for Rice and Thayers Lakes. In Rice Lake, macrophyte standing crops increased from winter to summer, but standing crops in July 2018 were 68% less than July 2017 (Figure 2.5a). In Thayers Lake, macrophyte standing crops increased 2-fold from summer 2017 to autumn 2017, decreased in the winter to amounts similar to summer 2017, then increased again in summer 2018 (Figure 2.5b). Stepwise multiple linear regression analysis did not produce a useful model for macrophyte standing crops considering predictors of water temperature and water clarity (Table 2.3). NMS ordination successional vectors between sampling timepoints show shifts in the macrophyte assemblage across the study period (Figure 2.4). In the ordination, the macrophyte assemblage in Thayers Lake had a similar position in ordination space during summer 2017 and summer of 2018. The macrophyte assemblage in Rice Lake from summer 2017 and summer 2018 show different positions in ordination space with higher values on Axis 1 in summer 2018 (Figure 2.4). In addition to changes in standing crops, macrophyte species richness was about half in the winter compared to the maximum (occurring in summer or autumn). Common over-wintering macrophytes were aquatic moss, *Chara* spp., *P. amplifolius*, and *M. humile* (Appendix G). Macrophyte species evenness in Rice Lake was 50% higher in the winter compared to other seasons, but only 12% higher in winter compared to other seasons in Thayers Lake (Appendix H).

Standing crops of other littoral primary producers changed seasonally across the study period in relation to environmental conditions and macrophyte standing crops. We

had hypothesized that epiphyte standing crops would mirror trends in macrophyte standing crops increasing in the summer and decreasing in the autumn. Standing crops of epiphyte Chla and epiphyte AFDM increased from spring to autumn, and decreased in the winter (Figure 2.5 c,d,e,f). AFDM of epiphytes was highest in Thayers Lake coincident with the highest macrophyte standing crops in autumn 2017. Linear regression and stepwise multiple linear regressions showed that epiphyte AFDM was positively related to macrophyte standing crops, but no models significantly explained variation in epiphyte Chla (Table 2.2, Table 2.3). Phytoplankton Chla in the winter was equal to 4-9% of the maximum standing crops (Figure 2.5 c,d). Stepwise multiple linear regression identified a significant positive relationship between water temperature and phytoplankton Chla, but no significant models for phytoplankton AFDM (Table 2.3). Benthic periphyton had the least variable Chla across seasons, with winter benthic periphyton Chla equal to 29% and 62% of the maximum Chla standing crops for Rice and Thayers Lakes, respectively (Figure 2.5 c,d). AFDM of benthic periphyton in Rice Lake was slightly higher during summer and autumn compared to winter (Figure 2.5 e,f). Linear regression and stepwise multiple linear regressions of benthic periphyton standing crops showed that benthic periphyton chla was positively related to macrophyte standing crops (Table 2.2, Table 2.3). No significant models were found for benthic periphyton AFDM (Table 2.2, Table 2.3).

2.3.3 Open water metabolism

Whole-plot rates of GPP and ER were lowest in the winter, and increased into the following summer. Winter rates of GPP were equal to 4% and 8% of the highest GPP

rates in Rice Lake and Thayers Lake, respectively. Winter ER rates were 4% of the highest ER rates in both lakes (Figure 2.6). In Rice Lake, GPP and ER were 44% and 64% lower in autumn 2017 than the summer 2018, while in Thayers Lake GPP and ER were 91% and 645% higher in autumn 2017 than the summer 2018 (Figure 2.6). Stepwise multiple linear regression identified significant models showing that both GPP and ER were positively related to water temperature and macrophyte standing crop, explaining 57-61% of the variation in rates (Figure 2.6, Table 2.3).

2.3.4 Primary production rates

GPP of primary producers were higher in the summer and autumn, and lowest in the winter. In both lakes, phytoplankton GPP was highest during the summer, while epiphyte GPP was highest in the autumn (Figure 2.7). GPP rates of zero occurred across seasons for phytoplankton in both lakes, and for epiphytes in July 2017 in Rice Lake (Figure 2.7). Epiphytes were not collected in the winter. Simple and multiple linear regressions of phytoplankton GPP identified that water temperature was positively related to and explained 34-38% of variance in phytoplankton GPP (Table 2.2), but did not identify any significant models for epiphyte GPP (Table 2.3).

2.4 Discussion

While studying primary producers in north-temperate lakes across a full year, we found that standing crops changed seasonally and GPP rates of plots and individual pri-

mary producer groups were positively related to water temperatures across seasons. Primary producers maintained standing crops all year, although standing crops were lower during winter. The highest rates of GPP were measured during the summer and autumn when water temperatures were 11.2 - 25.7 ºC, and at the lowest rates in the winter when water temperatures were between 0.8 - 3.4 ºC. We were limited in analysis and conclusions of primary producer GPP across all seasons due to errors that propagated in sampling methods, and limitations measuring primary production in the winter, in part due to hypoxia in the littoral zones of both lakes. Regardless, seasonal transitions of littoral primary producers and primary production was apparent in our study.

We hypothesized that standing crops of phytoplankton would increase during spring and autumn water column mixing periods. We also hypothesized that macrophyte and epiphyte standing crops would increase across the summer until autumn senescence, and benthic periphyton standing crop would decrease due to shading from macrophytes. Our sampling dates did not capture phytoplankton standing crops during water column mixing periods, yet we observed phytoplankton standing crops to be the lowest during winter. Similar to these observations, in a global meta-analysis of under-ice lake ecology, 50% of lakes had lower Chla in winter vs summer and their mean Chla was on average was 43% of the summer values (Hampton et al. 2016). Macrophyte standing crops were observed to be the highest in summer and autumn, and at the lowest in winter. Epiphyte standing crops were also high in summer and autumn, but were not collected in the winter due to difficulty collecting macrophytes in such a way that did not disturb attached algae.

Therefore, we were not able to assess our hypotheses about seasonal changes and epiphyte standing crop or GPP under the ice in this study.

Rates of GPP measured in this study were lowest in the winter and increased into the summer and autumn, and were significantly related to water temperatures. It is well established that temperature effects rates of biochemical reactions that comprise metabolic processes (Gillooly et al. 2001; Brown et al. 2004) and photosynthesis (Galmes et al. 2015). Drivers of metabolism in lakes depend on the temporal scale of analysis. At the daily scale, light and temperature are a primary control on GPP (Langman et al. 2010; Richardson et al. 2017), yet on the weekly scale storms events can be an important driver of GPP (Jennings et al. 2012). Seasonal changes to metabolism are largely driven by temperature and light (Hansen et al. 2006; Langman et al. 2010; Yvon-Durocher et al. 2010; Defore et al. 2016). In a detailed study of metabolism of a Danish lake, daily GPP values were strongly related to temperature, but GPP was seasonally dependent on temperature coupled with irradiance and primary producer biomass (Staehr and Sand-Jensen 2007). Similarly, a meta-analysis of pelagic production of 165 lakes mostly from the northern hemisphere found Chla specific production of lake phytoplankton decreased in lower water temperatures (range 5 - 25 ºC) (Morin et al. 1999). Globally, seasonal patterns of GPP and ER in lakes is common, yet not equally pronounced in all lakes closer to the equator or lakes with low trophic statuses (Solomon et al. 2013).

Our estimates of NPP and R using bottle assays during winter were hindered by methodological shortcomings and the physical properties of the systems we were sampling. In some lakes, oxygen concentrations slowly decrease through the winter under ice due to biological activity and sediment processes (Mathias and Barica 1980). Dissolved oxygen concentrations were 0.5 – 2.2 mg/L in Rice Lake and 1.2 – 3.4 mg/L in Thayers Lake during winter 2018. Water with low gas concentrations will readily absorb additional oxygen if exposed to the air, and this certainly occurred during the collection and preparation of BOD bottles containing primary producers as well as during analysis of gas concentrations with MIMS. This is supported by our observation that gas concentrations would increase when analyzing via MIMS before stabile readings could be achieved. We suspect this was a major source of error for all bottle estimates on sampling dates in February, March, and April. Future studies of under-ice processes in these lakes should use sampling protocols and equipment adapted for collecting anoxic samples that minimize air-gas exchange during handling (Welch 1974; Deshpande et al. 2015).

For a variety of reasons, what happens under the ice has often been dismissed as ecologically unimportant relative to the warmer summer growing periods, when most limnological research occurs (Powers and Hampton 2016). We found in the littoral zones of these north temperate lakes that rates of GPP and standing crops of all primary producers were lower in the winter than summer, but not absent or zero. Winter is often viewed as a season of suppression and a reset on the annual cycle, but it could also be an important time of transition for communities (Sommer et al. 2012). We detected in Thayers Lake that the macrophyte assemblage changed in the winter but transitioned back to a

similar assemblage the two summers we sampled. In Rice Lake, the macrophyte assemblage transitioned from the first summer to a new assemblage the second summer we sampled. We do not know the drivers of this assemblage shift, but winter conditions could play an important role. Another interesting finding was the presence of hypoxic and anoxic conditions that most likely extended into the sediments in the littoral zones of these lakes. The duration and spatial extent over which those conditions occur in each lake are unclear because we only sampled one location. Studies and observations of drivers and changes occurring because of, and under the ice, will offer great value to our understanding lake ecology, and could help predict ecosystem impacts from climate change in these aquatic systems.

3 References

APHA (2005) Standard Methods for the Examination of Water and Wastewater

Appling AP, Hall RO, Yackulic CB, Arroita M (2018) Overcoming Equifinality: Leveraging Long Time Series for Stream Metabolism Estimation. J Geophys Res Biogeosciences 123:624–645. doi: 10.1002/2017JG004140

Barko JW, Smart MR (1981) Sediment-based nutrition of submersed macrophytes. Aquat Bot 10:339–352

Barko JW, Smart MR, McFarland DG, Chen RL (1988) Interrelationships between the growth of Hydrilla verticillata (L.f.) Royle and sediment nutrient availability. Aquat Bot 32:205–216

Binzer T, Sand-Jensen K, Middelboe AL (2006) Community photosynthesis of aquatic macrophytes. Limnol Oceanogr 51:2722–2733. doi: 10.4319/lo.2006.51.6.2722

Boylen CW, Eichler LW, Madsen JD (1999) Loss of native plant species in a community dominated by Eurasian watermilfoil. Hydrobiologia 415:207–211. doi: 10.1023/A

Boylen CW, Sheldon RB (1976) Submergent macrophytes : growth under winter ice cover. Science (80-) 194:841–842

Brown JH, Gillooly JF, Allen AP, et al (2004) Toward a Metabolic Theory of Ecology. Ecology 85:1771–1789. doi: 10.1098/rstb.2003.1373

Burkholder JM, Wetzel RG (1990) Epiphytic alkaline phosphatase on natural and artificial plants in an oligotrophic lake : re-evaluation of the role of macrophytes as a phosphorus source for epiphytes. Limnol Oceanogr 35:736–747. doi: 10.4319/lo.1990.35.3.0736

Burnham KP, Anderson DR (2002) Model Selection and Multimodel Inference: A Practical Information-Theoretic Approach Second Edition, 2nd edn.

Carignan R, Blais A-M, Vis C (1998) Measurement of primary production and community respiration in oligotrophic lakes using the Winkler method. Can J Fish Aquat Sci 55:1078–1084

Carignan R, Kalff J (1982) Phosphorus release by submerged macrophytes: Significance to epiphyton and phytoplankton. Limnol Oceanogr 27:419–427. doi: 10.4319/lo.1982.27.3.0419

Carpenter SR, Lodge DM (1986) Effects of submerged macrophytes on ecosystem processes. Aquat Bot 26:341–370

Cattaneo A, Kalff J (1980) The relative contribution of aquatic macrophytes and their epiphytes to the production of macrophyte beds. Limnol Oceanogr 25:280–289. doi: 10.4319/lo.1980.25.2.0280

De Stasio BT, Hill DK, Kleinhans JM, et al (1996) Potential effects of global climate change on small north-temperate lakes: Physics, fish, and plankton. Limnol

Oceanogr 41:1136–1149. doi: 10.4319/lo.1996.41.5.1136

Defore A, Weinke A, Lindback M, Biddanda B (2016) Year-round measures of planktonic metabolism reveal net autotrophy in surface waters of a Great Lakes estuary. Aquat Microb Ecol. doi: 10.3354/ame01790

Deshpande BN, Macintyre S, Matveev A, Vincent WF (2015) Oxygen dynamics in permafrost thaw lakes: Anaerobic bioreactors in the Canadian subarctic. Limnol Oceanogr 60:1656–1670. doi: 10.1002/lno.10126

Dodds WK, Whiles MR (2010) Freshwater Ecology: Concepts and Environmental Applications of Limnology, 2nd edn. Academic Press

Fasset NC (1957) A Manual of Aquatic Plants, 2nd edn. The University of Wisconsin Press, Madison, Wisconsin

Ferreiro N, Giorgi A, Feijo C (2013) Effects of macrophyte architecture and leaf shape complexity on structural parameters of the epiphytic algal community in a Pampean stream. Aquat Ecol 47:389–401. doi: 10.1007/s10452-013-9452-1

Galmes J, Kapralov M V., Copolovici LO, et al (2015) Temperature responses of the Rubisco maximum carboxylase activity across domains of life: phylogenetic signals, trade-offs, and importance for carban gain. Photosynth Res 123:183–201

Gardner WS, McCarthy MJ, Carini SA, et al (2009) Collection of intact sediment cores with overlying water to study nitrogen- and oxygen-dynamics in regions with

seasonal hypoxia. Cont Shelf Res. doi: 10.1016/j.csr.2009.08.012

Gillooly JF, Brown JH, West GB, et al (2001) Effects of Size and Temperature on Metabolic Rate. Science (80-) 293:2248–2251. doi: 10.1126/science.1061967

Grutters BMC, Gross EM, van Donk E, Bakker ES (2017) Periphyton density is similar on native and non-native plant species. Freshw Biol 62:906–915. doi: 10.1111/fwb.12911

Hamme RC, Emerson SR (2004) The solubility of neon, nitrogen and argon in distilled water and seawater. Deep Res Part I Oceanogr Res Pap 51:1517–1528. doi: 10.1016/j.dsr.2004.06.009

Hampton SE, Galloway AWE, Powers SM, et al (2016) Ecology under lake ice. Ecol Lett 20:98–11. doi: 10.1111/ele.12699

Hansen GJA, Vander Zanden MJ, Blum MJ, et al (2013) Commonly Rare and Rarely Common: Comparing Population Abundance of Invasive and Native Aquatic Species. PLoS One 8:. doi: 10.1371/journal.pone.0077415

Hansen PC, Carpenter SR, Armstrong DE, et al (2006) Lake Dissolved Inorganic Carbon and Dissolved Oxygen: Changinge Drivers From Days to Decades. Ecol Monogr 76:343–363

Holmes RM, Aminot A, Kérouel R, et al (1999) A simple and precise method for measuring ammonium in marine and freshwater ecosystems. Can J Fish Aquat Sci

56:1801–1808. doi: 10.1139/f99-128

Horne AJ, Goldman CR (1994) Limnology, 2nd Editio. McGraw-Hill, Inc.

Hotchkiss ER, Hall RO (2015) Whole-stream ^{13}C tracer addition reveals distinct fates of newly fixed carbon. Ecology 96:403–416. doi: 10.1890/14-0631.1

Jackson DA, Harvey HH (1989) Biogeographic Associations in Fish Assemblages: Local vs. Regional Processes. Ecology 70:1472–1484

Jennings E, Jones S, Arvola L, et al (2012) Effects of weather-related episodic events in lakes: an analysis based on high-frequency data. Freshw Biol 57:589–601. doi: 10.1111/j.1753-318X.2010.01075.x/abstract

Jewell ME (1935) An Ecological Study of the Fresh-Water Sponges of Northeastern Wisconsin. Ecol Monogr 5:461–504

Johnson JA, Newman RM (2011) A comparison of two methods for sampling biomass of aquatic plants. J Aquat Plant Manag 49:1–8

Kana TM, Darkangelo C, Hunt MD, et al (1994) Membrane inlet mass spectrometer for rapid high-precision determination of N_2, O_2, and Ar in environmental water samples. Anal Chem 66:4166–4170. doi: 10.1021/ac00095a009

Keast A (1984) The introduced aquatic macrophyte, Myriophyllum spicatum, as habitat for fish and their invertebrate prey. Can J Zool 62:1289–1303

Kerfoot CW, Urban NR, McDonald CP, et al (2015) Legacy mercury releases during copper mining near Lake Superior. J Great Lakes Res 42:50–61. doi: 10.1016/j.jglr.2015.10.007

Kovalenko KE, Dibble ED (2014) Invasive macrophyte effects on littoral trophic structure and carbon sources. Hydrobiologia 721:23–34. doi: 10.1007/s10750-013-1633-3

Langman O, Hanson P, Carpenter S, Hu Y (2010) Control of dissolved oxygen in northern temperate lakes over scales ranging from minutes to days. Aquat Biol 9:193–202. doi: 10.3354/ab00249

Larue EA, Zuellig MP, Netherland MD, et al (2013) Hybrid watermilfoil lineages are more invasive and less sensitive to a commonly used herbicide than their exotic parent (Eurasian watermilfoil). Evol Appl 6:462–471. doi: 10.1111/eva.12027

Lassen C, Revsbech NP, Pedersen O (1997) Macrophyte developement and resuspension regulate the photosynthesis and production of benthic microalgae. Hydrobiologia 350:1–11. doi: https://doi.org/10.1023/A:1003052226202

Lauster GH, Hanson PC, Kratz TK (2006) Gross primary production and respiration differences among littoral and pelagic habitats in northern Wisconsin lakes. Can J Fish Aquat Sci 63:1130–1141. doi: 10.1139/f06-018

Liboriussen L, Jeppesen E (2003) Temporal dynamics in epipelic, pelagic and epiphytic

algal production in a clear and a turbid shallow lake. Freshw Biol 48:418–431. doi: 10.1046/j.1365-2427.2003.01018.x

Madsen JD, Boylen CW (1989) Eurasian watermilfoil seed ecology from an oligotrophic and eutrophic lakes. J. Aquat. Plant Manag. 27:119–121

Madsen JD, Sutherland JW, Bloomfield JA, et al (1991) Decline of native vegetation under dense eurasion watermilfoil canopies. J Aquat Plant Manag 29:94–99

Magnuson JJ (2009) Historical trends in lake and river ice cover in the northern hemisphere. Science (80-) 289:1743–1746. doi: 10.1126/science.289.5485.1743

Marcarelli AM, Wurtsbaugh WA (2009) Nitrogen Fixation Varies Spatially and Seasonally in Linked Stream-Lake Ecosystems. Biogeochemistry 94:95–110. doi: 10.1007/s10533-009-931

Mathias JA, Barica J (1980) Factors Controlling Oxygen Depletion in Ice-Covered Lakes. Can J Fish Aquat Sci 37:185–194. doi: Doi 10.1139/F80-024

McCune B, Grace JB (2002) Analysis of Ecological Communities. MjM Software Design, Gleneden Beach, Oregon

McCune B, Mefford MJ (2011) PC-ORD

McCune B, Mefford MJ (2018) PC-ORD

Michigan Department of Natural Resources (2018) Inland Lake Maps. In: Website.

https://www.michigan.gov/dnr/0,4570,7-350-79119_79146_81198_85509---,00.html. Accessed 15 Sep 2018

Michigan State University (2018) Midwest Invasive Species Information Network. https://www.misin.msu.edu/

Michigan Technological University, LimnoTech, Great Lakes Observing System (2018) Upper Great Lakes Observing System. http://uglos.mtu.edu/. Accessed 16 Sep 2018

Moody ML, Les DH (2007) Geographic distribution and genotypic composition of invasive hybrid watermilfoil (Myriophyllum spicatum x M. sibiricum) populations in North America. Biol Invasions 9:559–570. doi: 10.1007/s10530-006-9058-9

Moody ML, Palomino N, Weyl PSR, et al (2016) Unraveling the biogeographic origins of the Eurasian watermilfoil (Myriophyllum spicatum) invasion in North America. Am J Bot 103:709–718. doi: 10.3732/ajb.1500476

Morin A, Lamoureux W, Busnarda J (1999) Empirical Models Predicting Primary Productivity from Chlorophyll a and Water Temperature for Stream Periphyton and Lake and Ocean Phytoplankton. J North Am Benthol Soc 18:299–307

Navionics Navionics Charviewer. https://webapp.navionics.com

Nichol SA, Shaw BH (1986) Ecological life histories of the three aquatic nuisance plants, Myriophyllum spicatum, Potamogeton crispus and Elodea canadensis. Hydrobiologia 131:3–21

NOAA (2018) NOAA Solar Calculator. https://www.esrl.noaa.gov/gmd/grad/solcalc/

Parkinson H, Mangold J, Jacobs J, et al (2011) Biology, Ecology and Management of Eurasian WaterMilfoil. http://msuextension.org/publications/AgandNaturalResources/EB0193.pdf

Parks SR, McNair JN, Hausler P, et al (2017) Divergent responses of cryptic invasive watermilfoil to treatment with auxinic herbicides in a large Michigan Lake. Lake Reserv Manag 32:366–372. doi: 10.1080/10402381.2016.1212955

Powers SM, Hampton SE (2016) Winter Limnology as a New Frontier. Limnol Oceanogr Bull 25:103–108. doi: 10.1002/lob.10152

R Core Team (2018) R: A Language and Environment for Statistical Computing

Reuter JE, Axler RP (1992) Physiological characteristics of inorganic nitrogen uptake by spatially separate algal communitites in a nitrogendeficient lake. Freshw Biol 27:227–236

Richardson DC, Carey CC, Bruesewitz DA, Weathers KC (2017) Intra- and inter-annual variability in metabolism in an oligotrophic lake. Aquat Sci 79:319–333. doi: 10.1007/s00027-016-0499-7

Scheffer M (1998) Ecology of Shallow Lakes. Chapman & Hall, London

Scheffer M, Hosper SH, Meijer M-L, et al (1993) Alternative equilibria in shallow lakes. Trends Ecol Evol 8:275–279

Sher-Kaul S, Oertli B, Castella E, Lachavanne J-B (1995) Relationship between biomass and surface area of six submerged aquatic plant species. Aquat Bot 51:147–154

Skawinski PM (2014) Aquatic Plants of the Upper Midwest: A photographic field guide to our underwater forests, 2nd edn. Wisconsin, USA

Smith CS, Barko JW (1990) Ecology of Eurasian watermilfoil. J Aquat Plant Manag 28:55–64

Solomon CT, Bruesewitz DA, Richardson DC, et al (2013) Ecosystem respiration: Drivers of daily variability and background respiration in lakes around the globe. Limnol Oceanogr 58:849–866. doi: 10.4319/lo.2013.58.3.0849

Sommer U, Adrian R, De Senerpont Domis L, et al (2012) Beyond the Plankton Ecology Group (PEG) Model: Mechanisms Driving Plankton Succession. Annu Rev Ecol Evol Syst 43:120913143848009. doi: 10.1146/annurev-ecolsys-110411-160251

Sommer U, Gliwicz ZM, Lampert W, Duncan A (1986) The PEG*-model of seasonal succession of planktonic events in fresh water. Arch Hydrobiol 106:433–471. doi: 10.1111/j.1469-185X.1969.tb01218.x

Staehr PA, Sand-Jensen K (2007) Temporal dynamics and regulation of lake metabolism. Limnol Oceanogr 52:108–120. doi: 10.4319/lo.2007.52.1.0108

Stan Development Team (2018) RStan: the R interface to Stan

Taylor BW, Keep CF, Hall RO, et al (2007) Improving the fluorometric ammonium

method: matrix effects, background fluorescence, and standard additions. J North Am Benthol Soc 26:167–177. doi: 10.1899/0887-3593(2007)26[167:ITFAMM]2.0.CO;2

Taylor JR (1982) An Introduction to Error Analysis: The Study of Uncertainties in Physical Measurements, 2nd edn. University Science Books, Sausalito, CA

Thum RA, Parks S, Mcnair JN, et al (2017) Note Survival and vegetative regrowth of Eurasian and hybrid watermilfoil following operational treatment with auxinic herbicides in Gun Lake , Michigan. 103–107

Trebitz AS, Taylor D. (2007) Exotic and invasive aquatic plants in Great Lakes coastal wetlands: Distribution and relation to watershed land use and plant richness and cover. J Great Lakes Res 33:705–721. doi: 10.3394/0380-1330(2007)33

USEPA (1993a) Method 365.1, Revision 2.0: Determination of Phosphorus by Semi-Automated Colorimetry

USEPA (1993b) Method 353.2, Revision 2.0: Determination of Nitrate-Nitrite Nitrogen by Automated Colorimetry

Vadeboncoeur Y, Kalff J, Christoffersen K, Jeppesen E (2006) Substratum as a driver of variation in periphyton chlorophyll and productivity in lakes. J North Am Benthol Soc 25:379–392

Vadeboncoeur Y, Lodge DM, Carpenter SR (2001) Whole-Lake Fertilization Effects On

Distribution Of Primary Production Between Benthic And Pelagic Habitats. Ecology 82:1065–1077

Vadeboncoeur Y, McIntyre PB, Vander Zanden MJ (2011) Borders of biodiversity: life at the edge of the world's large lakes. Bioscience 61:526–537. doi: 10.1525/bio.2011.61.7.7

Vadeboncoeur Y, Steinman AD (2002) Periphyton function in lake ecosystems. TheScientificWorld 2:1449–1468. doi: 10.1100/tsw.2002.294

Van de Bogert MC, Bade DL, Carpenter SR, et al (2012) Spatial heterogeneity strongly affects estimates of ecosystem metabolism in two north temperate lakes. Limnol Oceanogr 57:1689–1700. doi: 10.4319/lo.2012.57.6.1689

Van de Bogert MC, Carpenter SR, Cole JJ, Pace ML (2007) Assessing pelagic and benthic metabolism using free water measurements. Limnol Oceanogr Methods 5:145–155

Vis C, Hudon C, Carignan R (2006) Influence of the vertical structure of macrophyte stands on epiphyte community metabolism. Can J Fish Aquat Sci 63:1014–1026. doi: 10.1139/f06-021

Vollenweider RA, Talling JF, Westlake DF (1969) a Manual on Methods for Measuring Primary Production in Aquatic Environments, IBP Handbo. F.A. Davis Company, Philadelphia

Welch E (1974) Metabolic rates of arctic lakes. Limnol Oceanogr 19:65–73

Wetzel RG, Likens GE (2000) Primary Productivity of Phytoplankton. In: Limnological Analyses, 2nd edn. Springer-Verlag, p 219–239.

Wetzel RG, Rich PH, Miller MC, Allen HL (1972) Metabolism of dissolved and particulate organic carbon in a temperate hard-water lake. W. K. Kellogg Biological Station, Hickory Corners, pp 1–115

Winslow LA, Zwart JA, Batt RD, et al (2016) LakeMetabolizer: An R package for estimating lake metabolism from free-water oxygen using diverse statistical models. Inl Waters 6:622–636. doi: 10.5268/IW-6.4.883

Yvon-Durocher G, Allen AP, Montoya JM, et al (2010) The temperature dependence of the carbon cycle in aquatic ecosystems

4 Tables

Table 1.1: Locations and physical descriptions of waterbodies and study plots

Waterbody	Abbreviation	Area (km^2)	Maximum Depth (m)	Mean Depth (m)	Plot type	Coordinates (latitude, longitude)	Plot depth (m)
Horseshoe Lake	HSL	0.15	11	3	UNINV	44.415065, -84.277678	1.6
					INV	44.417395, -84.281130	2.1
Lake St. Helen	STHL	9.70	8	2	UNINV	44.370373, -84.497893	1.4
					INV	44.369626, -84.499011	1.7
Islington Bay of Lake Huron	LCI	1.61*	4	2	UNINV	45.977832, -84.358537	2.5
					INV	45.973228, -84.353715	2.6
Sturgeon Sloughs of Portage Lake	SLG	0.96*	9	2	UNINV	47.032063, -88.485310	1.3
					INV	47.031971, -88.485941	1.2
Iron Lake	IRL	1.60	17	6	UNINV	46.149005, -88.641917	1.5
					INV	46.151059, -88.644730	2.4
Torch Lake	TCH	11.00	37	15	UNINV	47.133131, -88.457900	2.2
					INV	47.133346, -88.458414	2.3

Physical descriptions of lakes were determined from measuring and visually interpreting bathymetric lake maps (Navionics; Michigan Department of Natural Resources 2018). Physical descriptions of Torch Lake from (Kerfoot et al. 2015).
* area of open water around plot location reported instead of full waterbody area due to a greater relevance of physical parameters to site conditions.

Table 1.2: Two-sided paired t-tests results for invaded vs. uninvaded plots

Parameter	t-value	Degrees freedom	p- value
Depth	2.05	5	0.10
Light extinction coefficient	-2.01	5	0.10
Water temperature	-0.01	5	0.99
%ODO	0.89	5	0.45
Conductivity	-1.46	5	0.20
TDN	-0.23	5	0.83
DOC	-1.61	5	0.17
NH_4^+	-0.07	5	0.95
SRP	0.02	5	0.98
Macrophyte species richness	0.88	5	0.42
Macrophyte species evenness	1.58	5	0.17
Macrophyte Shannon's diversity	1.40	5	0.22
Macrophyte Simpson's diversity	1.21	5	0.28

Positive t-values indicate greater values in invaded plots

Table 1.3: Dominance of IWM at plots by abundance in each plot and standardized abundance

Waterbody	Plot type	Upper water column of IWM	Abundance of IWM in plots (%)	Standardized abundance of IWM (%)
HSL	UNINV	NA	4	2
	INV	Sparse	84	7
STHL	UNINV	NA	0	0
	INV	Sparse	35	23
LCI	UNINV	NA	0	0
	INV	Dense	65	30
SLG	UNINV	NA	0	0
	INV	Sparse	27	15
IRL	UNINV	NA	5	2
	INV	Dense	68	56
TCH	UNINV	NA	0	0
	INV	Dense	89	52

Standardized abundance was calculated as standing crop of IWM divided by the maximum standing crop value of a macrophyte species (294 g/m^2)
NA = not applicable

Table 1.4: Stepwise multiple linear regression models selected for responses of primary producers across all plots. Best models were selected for fit and parsimony by examining Akaike Information Criterion (AIC) scores

	Coefficients of Predictors										
Response	Light extinction	Water temperature	TDN	Macrophyte standing crop	Epiphyte Chla†	Phytoplankton AFDM	Intercept	Adjusted R^2	F	df	p
Benthic Periphyton GPP		23.056		-0.64	*	*	-342.15	0.50	6.54	2,9	**0.02**
Epiphyte GPP			-181.86	0.21	*	*	111.17	0.21	2.48	2,9	0.14
Phytoplankton GPP		13.86			*	*	-251.35	0.46	10.34	1,10	**0.009**
Benthic Periphyton Chla†		0.11		-0.003	*	*	-0.12	0.49	6.25	2,9	**0.02**
Epiphyte Chla†			-1.48	0.002	*	*	1.20	0.20	2.41	2,9	0.15
Phytoplankton Chla†			1.40	0.001	*	*	-0.24	0.65	11.06	2,9	**0.004**
Benthic Periphyton AFDM†	-0.21			0.001	*	*	2.39	0.47	5.89	2,9	**0.02**
Epiphyte AFDM			-16.89	0.02	*	*	10.44	0.20	2.39	2,9	0.15
Phytoplankton AFDM		0.95			*	*	-15.33	0.30	5.70	1,10	**0.04**
Plot GPP†						*	NA	NA	NA	NA	NA
Plot ER‡†		-0.08			*		2.51	0.25	4.66	1,10	0.06

Chla = chlorophyll a
AFDM = ash free dry mass
GPP = gross primary productivity
ER = ecosystem respiration
df = degrees freedom
† log transformed
‡ Converted to positive values from negative values
predictor not included in lowest AIC scored model
* not included as a predictor for multiple linear regression analysis
NA = not applicable, no model produced

Table 2.1: Locations, physical, and water characteristics of plots across sample dates

Lake (Latitude, Longitude)	Sample Date	Water + ice depth (m)	Conductivity (mS cm^{-1})	Light extinction coefficient	DOC (mg/L)	TDN (mg/L)	NH_4^+ (µg/L)	NO_3^-+NO_2^- (µg/L)	SRP (µg/L)
Thayers Lake (47.287142, -88.258384)	5/19/2017	1.60	0.020	1.398	11.59	0.339	1.8	1.6	0.9
	6/28/2017	1.76	0.020	1.368	14.30	0.408	4.0	5.0	0.9
	10/08/2017	1.68	0.079	1.940	13.14	0.443	8.5	1.6	0.9
	3/22/2018	0.83 + 0.75	0.540	1.815	–	–	74.6	30.0	0.9
	4/20/2018	0.77 + 0.75	0.510	1.277	–	–	35.3	53.0	3.6
	5/27/2018	1.49	0.023	–	–	–	2.0	14.0	0.9
	7/22/2018	1.49	0.060	1.867	16.12	0.450	3.8	1.6	0.9
Rice Lake (47.161358, -88.280696)	7/02/2017	1.58	–	2.571	15.11	0.389	20.6	25.0	6.6
	9/10/2017	1.69	–	1.622	13.31	0.420	12.5	1.6	0.9
	10/17/2017	1.39	0.045	1.922	12.25	0.417	9.6	31.0	0.9
	2/22/2018	0.92 + 0.5	0.046	2.218	–	–	19.4	1.6	6.7
	3/08/2018	0.92 + 0.5	0.046	1.689	13.78	0.504	27.0	1.6	0.9
	4/05/2018	0.75 + 0.6	0.510	1.288	–	–	8.2	209.0	0.9
	5/29/2018	1.6	–	–	12.24	0.356	3.0	1.6	0.9
	7/14/2018	1.53	0.029	2.401	–	–	46.8	31.0	0.9

Sample dates where measurements are missing is indicated by a dash (–)

Table 2.2: Simple linear regression models of primary producer responses for predictors across all plots.

	Coefficients of Predictors							
Response	Percent light at 1m depth	Water Temperature	Macrophyte standing crop†	Intercept	Multiple R^2	F	DF	p
Phytoplankton GPP	336.01	▯	▯	-92.48	0.13	1.53	1,10	0.24
Phytoplankton GPP	▯	45.32	▯	-517.46	0.38	7.30	1,12	**0.02**
Epiphyte GPP	185.60	▯	▯	-14.10	0.05	0.27	1,5	0.63
Epiphyte GPP	▯	-7.82	▯	272.83	0.07	0.55	1,7	0.48
Epiphyte Chla†	▯	▯	0.71	-0.78	0.29	2.92	1,7	0.13
Epiphyte AFDM†	▯	▯	1.00	-1.23	0.69	15.70	1,7	**0.005**
Benthic Periphyton Chla†	▯	▯	0.74	0.42	0.52	12.05	1,11	**0.005**
Benthic Periphyton AFDM	▯	▯	23.26	216.30	0.06	0.76	1,11	0.40

Chla = chlorophyll a
AFDM = ash free dry mass
GPP = gross primary productivity
DF = degrees freedom
† log transformed
▯ predictor not included in model

Table 2.3: Stepwise multiple linear regression models selected for responses of primary producers across all plots. Best models were selected for fit and parsimony by examining Akaike Information Criterion (AIC) scores.

	Coefficients of Predictors								
Response	Light Extinction	Water Temperature	Macrophyte standing crop†	Benthic Periphyton AFDM	Intercept	Adjusted R^2	F	DF	*p*
Epiphyte GPP	□	□	294.8	*	-293.8	0.33	3.99	1,5	0.10
Phytoplankton GPP	□	47.63	□	*	-661.33	0.34	6.25	1,9	**0.03**
Benthic Periphyton Chla†	□	□	0.75	*	0.41	0.44	8.69	1,9	**0.02**
Epiphyte Chla†	□	-0.06	□	*	1.43	0.27	3.21	1,5	0.13
Phytoplankton Chla†	□	0.03	□	*	-0.05	0.35	5.86	1,8	**0.04**
Benthic Periphyton AFDM	□	□	□	*	NA	NA	NA	NA	NA
Epiphyte AFDM†	□	□	1.00	*	-1.15	0.78	22.11	1,5	**0.005**
Phytoplankton AFDM†	-0.38	0.01	□	*	1.10	0.43	3.98	2,6	0.08
Macrophyte standing crop	□	□	*	*	NA	NA	NA	NA	NA
Plot GPP	□	0.07	0.78	*	-0.76	0.57	6.99	2,7	**0.02**
Plot ER‡†	□	0.07	0.82	-0.01	-0.40	0.61	5.66	3,6	**0.03**

Chla = chlorophyll a
AFDM = ash free dry mass
GPP = gross primary productivity
ER = ecosystem respiration
DF = degrees freedom
† log transformed
‡ Converted to positive values from negative values
□ predictor not included in lowest AIC scored model
* not included as a predictor for multiple linear regression analysis
NA = not applicable, no model produced

5 Figures

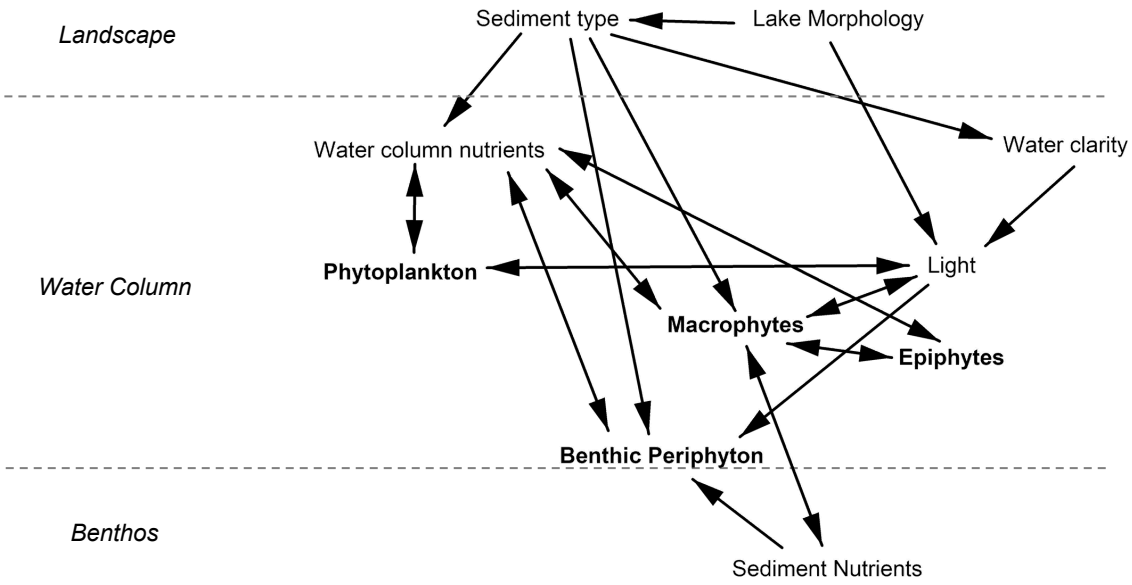

Figure 1.1: Interactions among littoral primary producers and their limiting resources in lakes. Hierarchical levels are labeled in italics (left) and area delineated by horizontal dashed lines. Primary producers are in bold. Arrows determine directions of interactions among entities but do not differentiate between positive or negative effects.

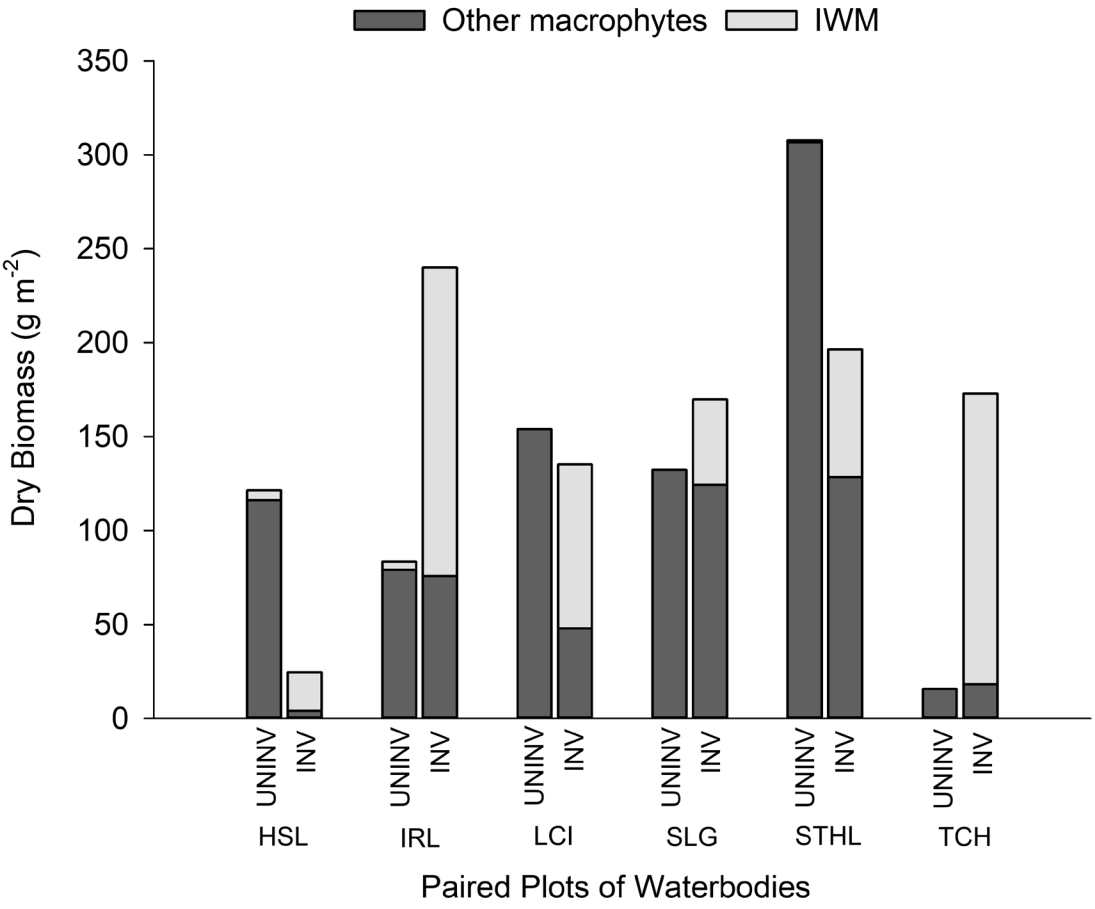

Figure 1.2: Mean standing crops of macrophytes in paired invaded (INV) and uninvaded (UNINV) plots, scaled per m^2 of plot surface area. Other macrophytes represents the sum of mean standing crops of all native macrophyte species in each plot.

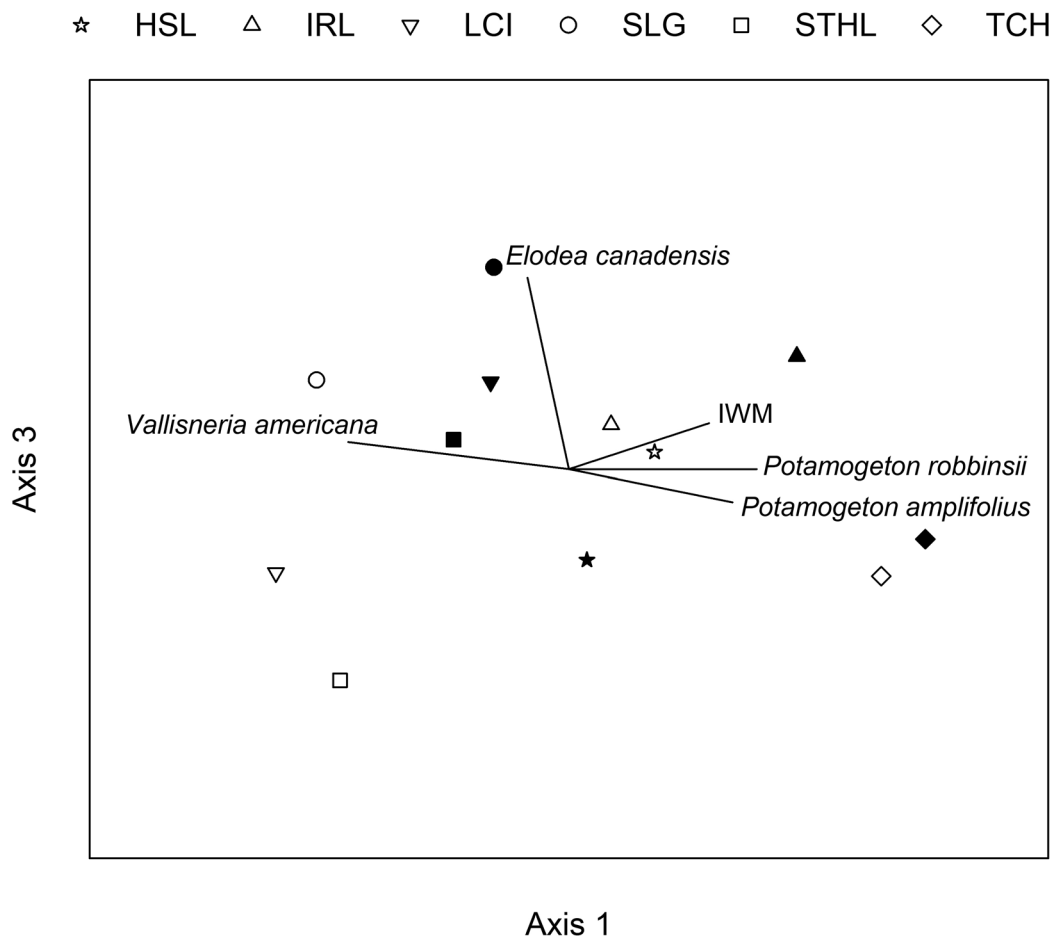

Figure 1.3: NMS ordination of paired plots in species space. Shaded symbols represent invaded plots and unshaded symbols represent uninvaded plots for each respective waterbody (different shape for each; abbreviations in Table 1.1). Lines represent joint plots of macrophyte species variables (r^2 cutoff = 0.40, Appendix F). Species shown are *Vallisneria americana* (Axis 1 R^2 = 0.69, Axis 3 R^2 = 0.10), *Elodea canadensis* (Axis 1 R^2 = 0.01, Axis 3 R^2 = 0.74), IWM (Axis 1 R^2 = 0.44, Axis 3 R^2 = 0.18), *Potomogeton robbinsii* (Axis 1 R^2 = 0.59, Axis 3 R^2 = 0.00), and *P. amplifolius* (Axis 1 R^2 = 0.51, Axis 3 R^2 = 0.13). Not shown are *Chara* spp. (Axis 2 R^2 = 0.50), *P. zosteriformis* (Axis 2 R^2 = 0.45), and *Najas guadalupensis* (Axis 2 R^2 = 0.50).

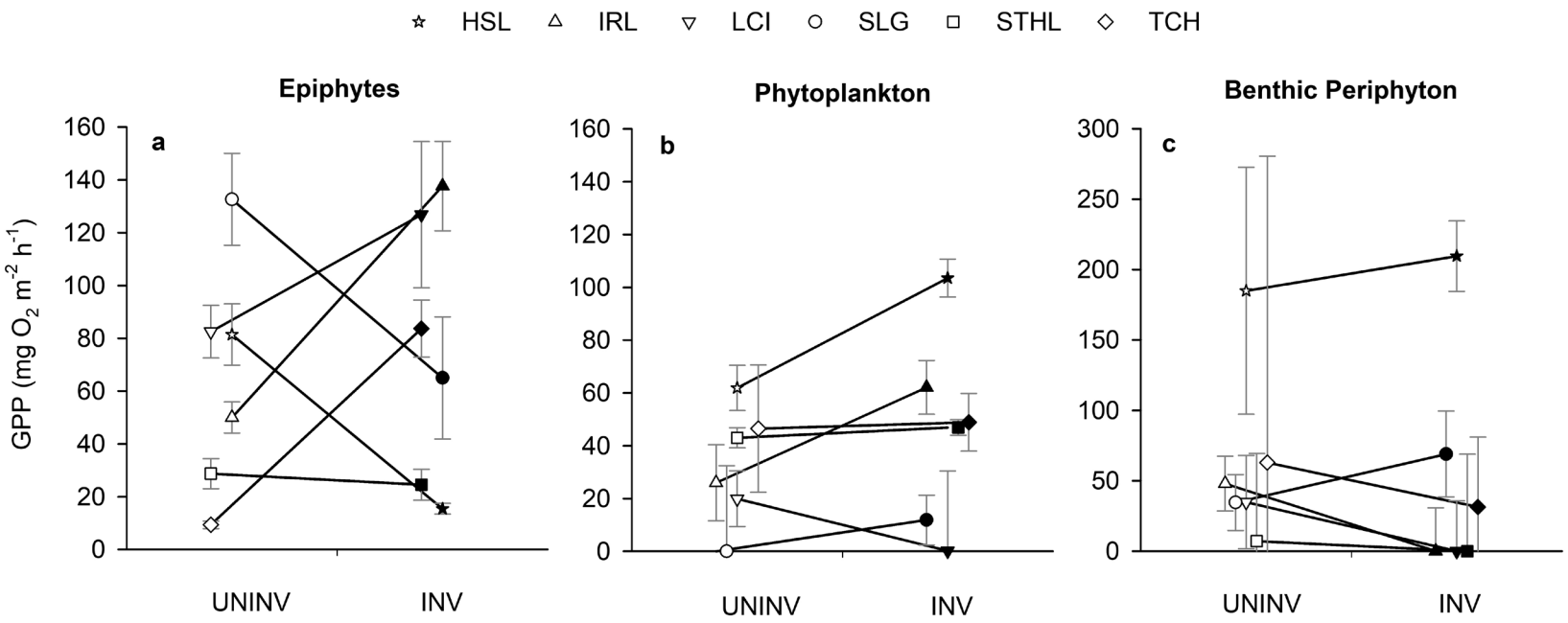

Figure 1.4: GPP measured in light-dark bottles and scaled per plot area of (**a**) epiphytes, (**b**) phytoplankton, and (**c**) benthic periphyton. Means ± 1SE are represented by symbols with error bars. Shaded symbols represent invaded plots and unshaded symbols represent uninvaded plots for each respective waterbody (different shape for each; abbreviations in Table 1.1). Lines connecting symbols illustrate differences in paired invaded (INV) and uninvaded (UNINV) plots. Symbols are offset horizontally to aid in interpretation of error bars.

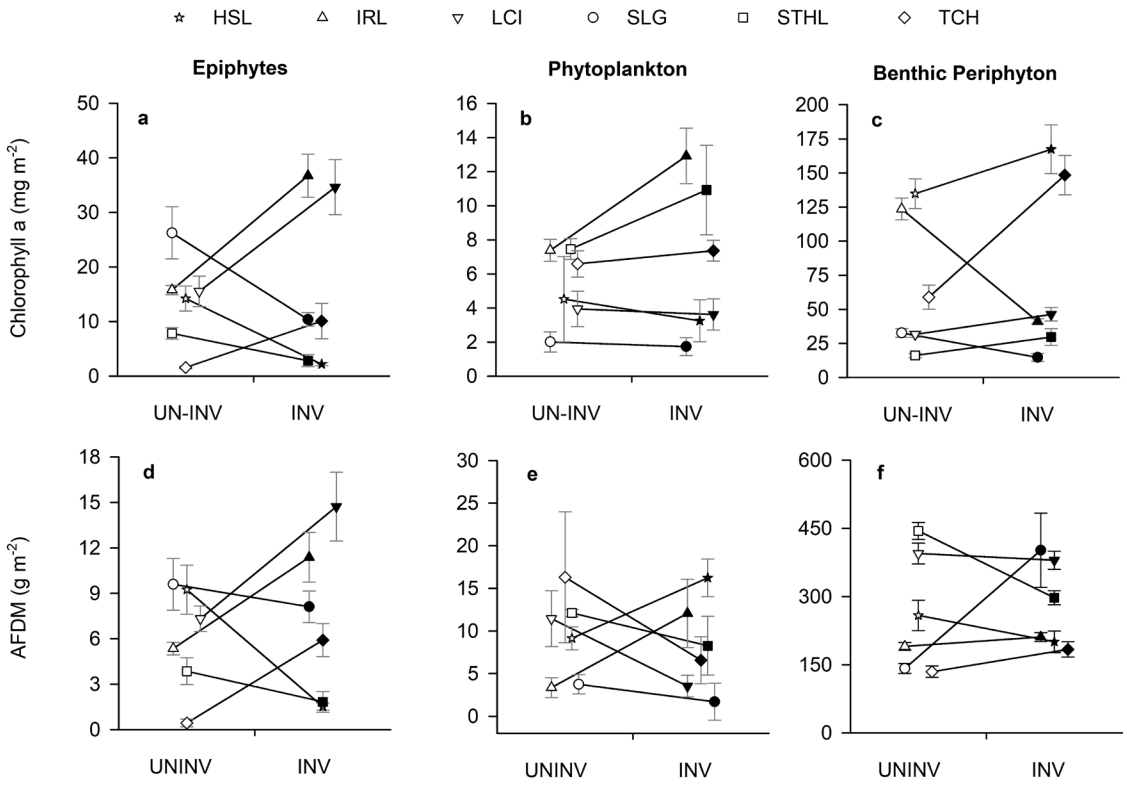

Figure 1.5: Standing crops of chlorphyll a and ash free dry mass (AFDM) for (**a**,**d**) epiphytes, (**b**,**e**) phytoplankton, and (**c**,**f**) benthic periphyton. Means ± 1SE are represented by symbols with error bars. Shaded symbols represent invaded plots and unshaded symbols represent uninvaded plots for each respective waterbody (different shape for each; abbreviations in Table 1.1). Lines connecting symbols illustrate differences in paired invaded (INV) and uninvaded (UNINV) plots. Symbols are offset horizontally to aid in interpretation of error bars.

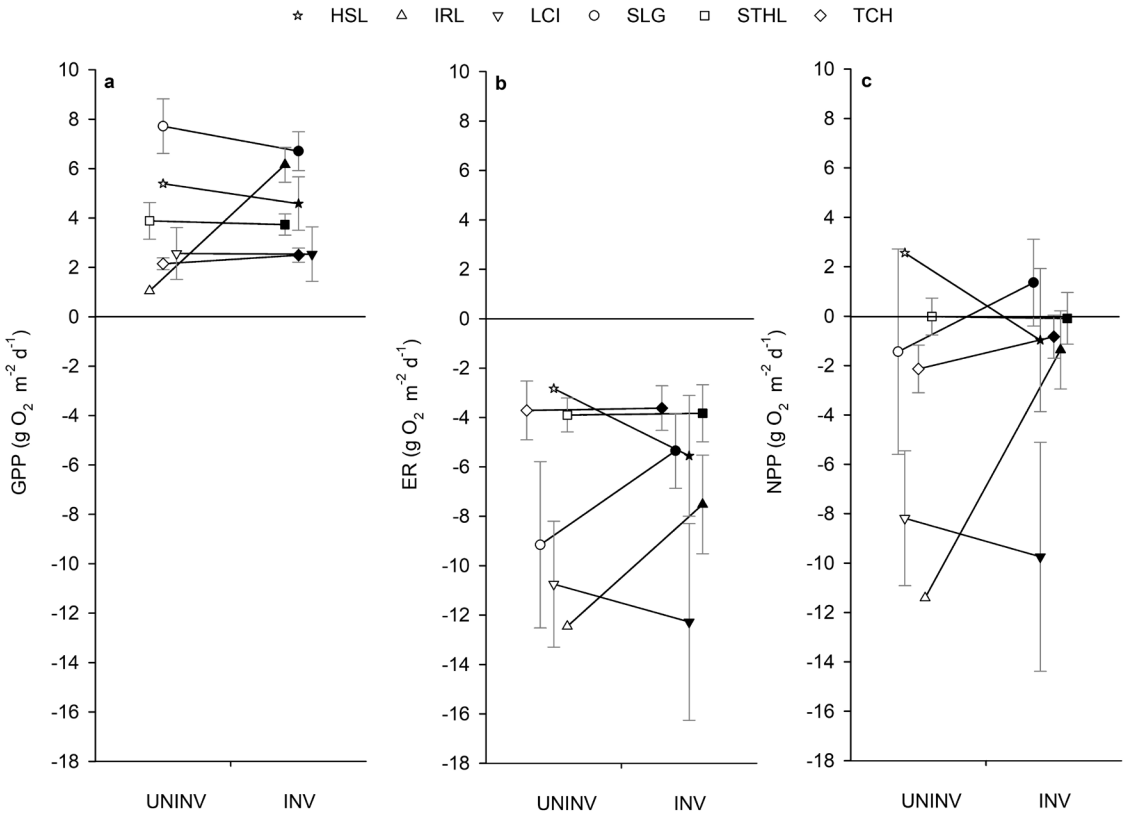

Figure 1.6: Mean (**a**) GPP, (**b**) ER, and (**c**) NPP rates of paired invaded (INV) and uninvaded (UNINV) plots measured using the open-water technique and averaged over deployment periods. Means ± 1SE are represented by symbols with error bars. Shaded symbols represent invaded plots and unshaded symbols represent uninvaded plots for each respective waterbody (different shape for each; abbreviations in Table 1.1). Lines connecting symbols illustrate differences in paired plots. Symbols are offset horizontally to aid in interpretation of error bars.

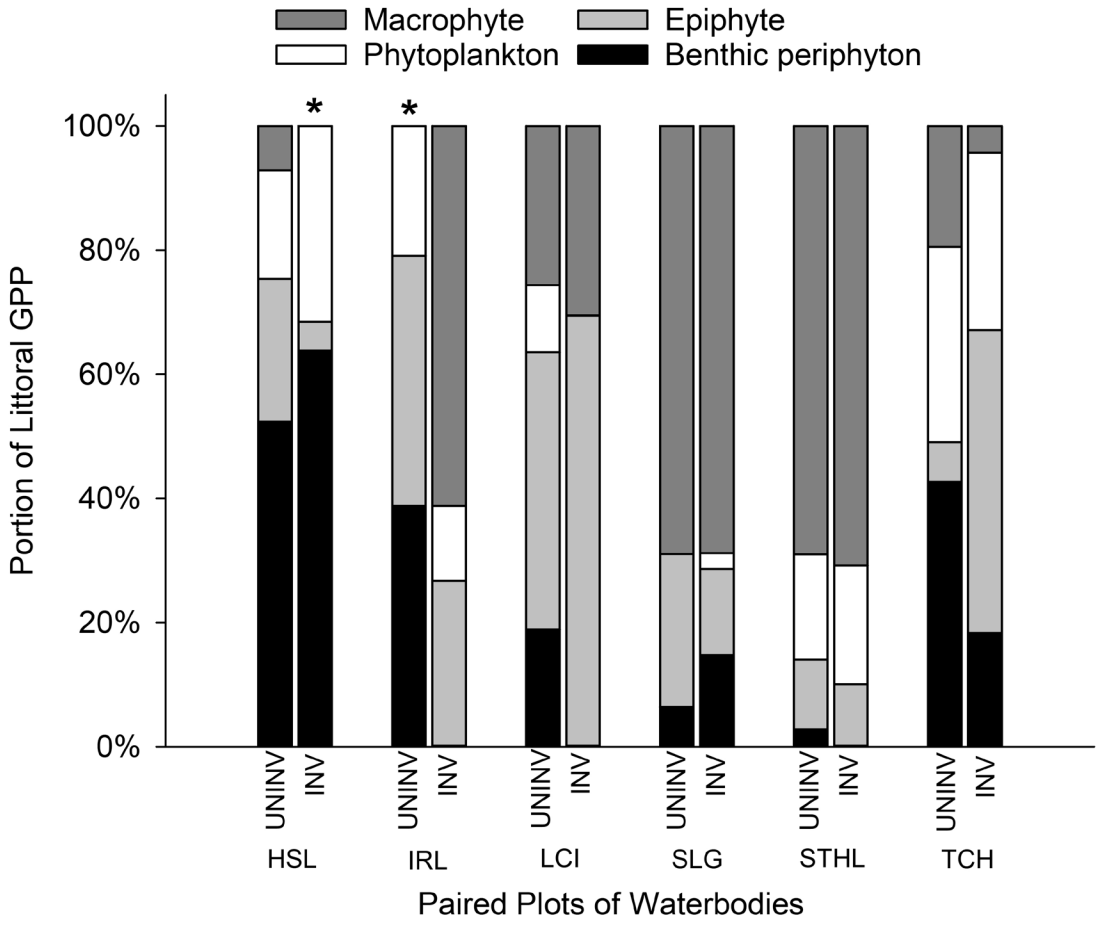

Figure 1.7: Portions of plot GPP by epiphytes, phytoplankton, benthic periphyton, and estimated macrophytes in paired invaded (INV) and uninvaded (UNINV) plots. Portions of GPP from macrophytes that were set to zero are indicated with (*); see section 1.2.6 for related methods.

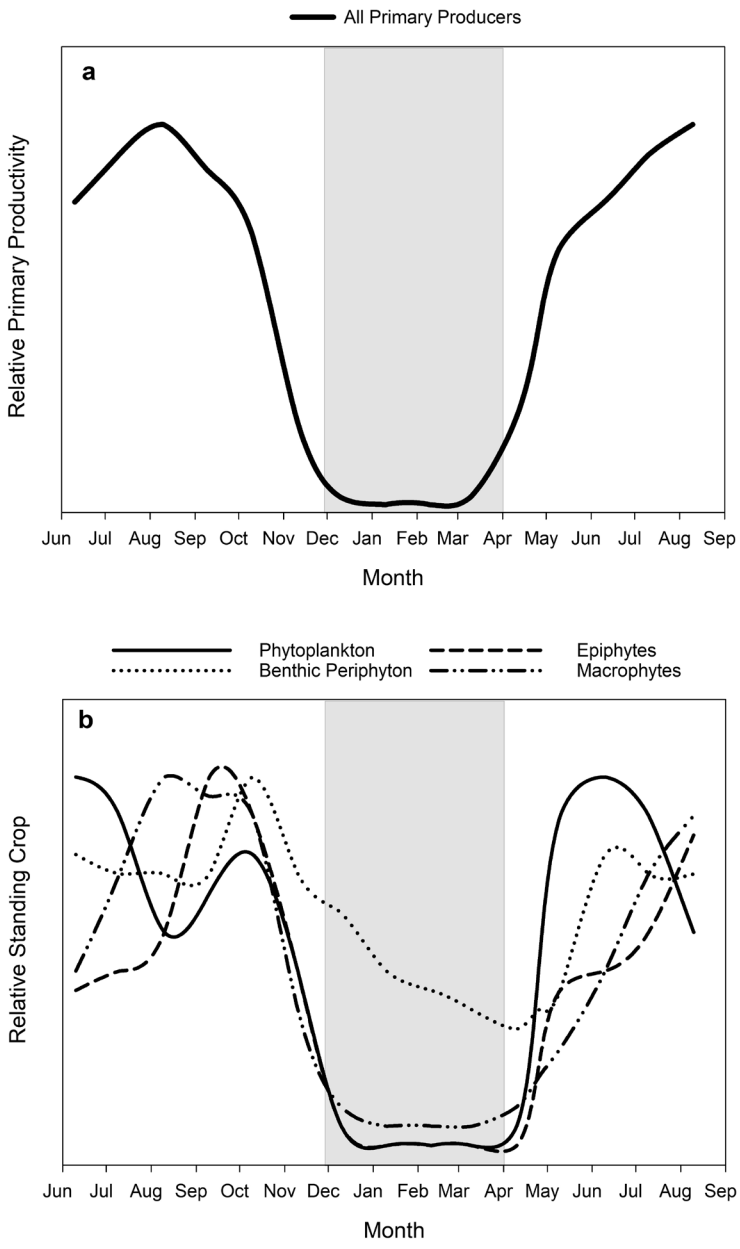

Figure 2.1: Hypothesized trends of the combined productivity of all primary producers (**a**) and standing crops of littoral primary producers (**b**) across a typical year in north-temperate lakes. The shaded background indicates when lakes would have ice cover.

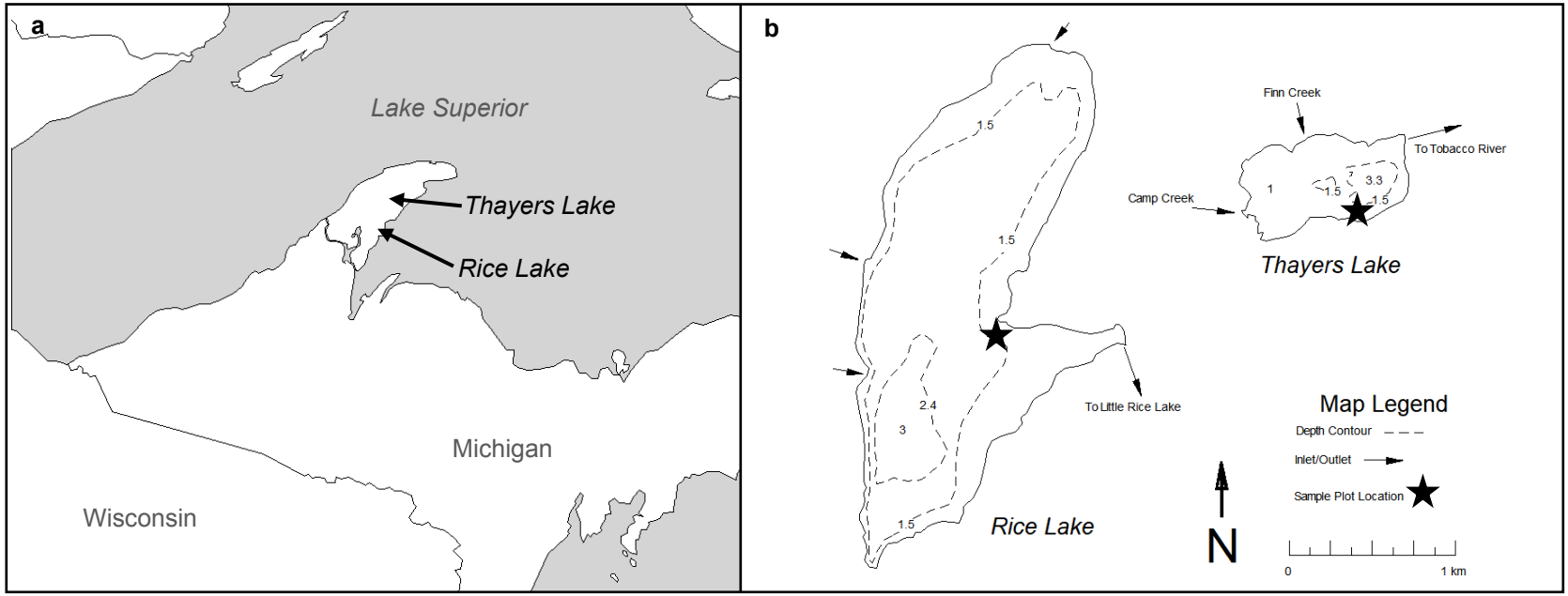

Figure 2.2: Location of Rice and Thayers Lake in the Upper Peninsula of Michigan (**a**). Bathymetric maps and study locations of Rice and Thayers Lake (b). Lakes are drawn to scale, but true distance between lakes is not represented in (**b**). Depth contours are labeled in meters and adapted from Michigan DNR inland lake maps (2018).

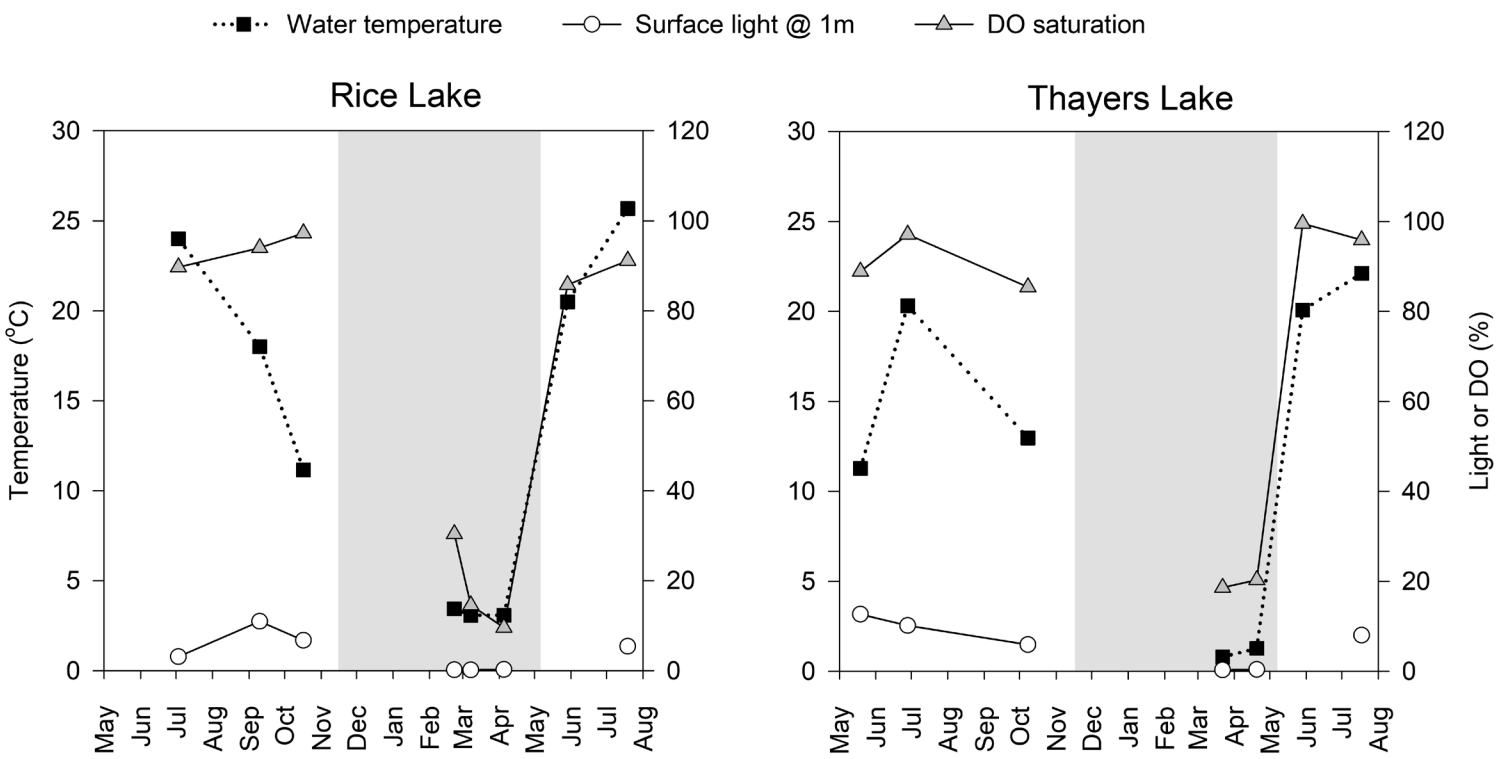

Figure 2.3: Physical characteristics of plots from summer 2017 to summer 2018. The surface light detected at 1m depth and DO saturation are reported as percent on the second y-axis. The shaded background indicates when lakes had ice cover.

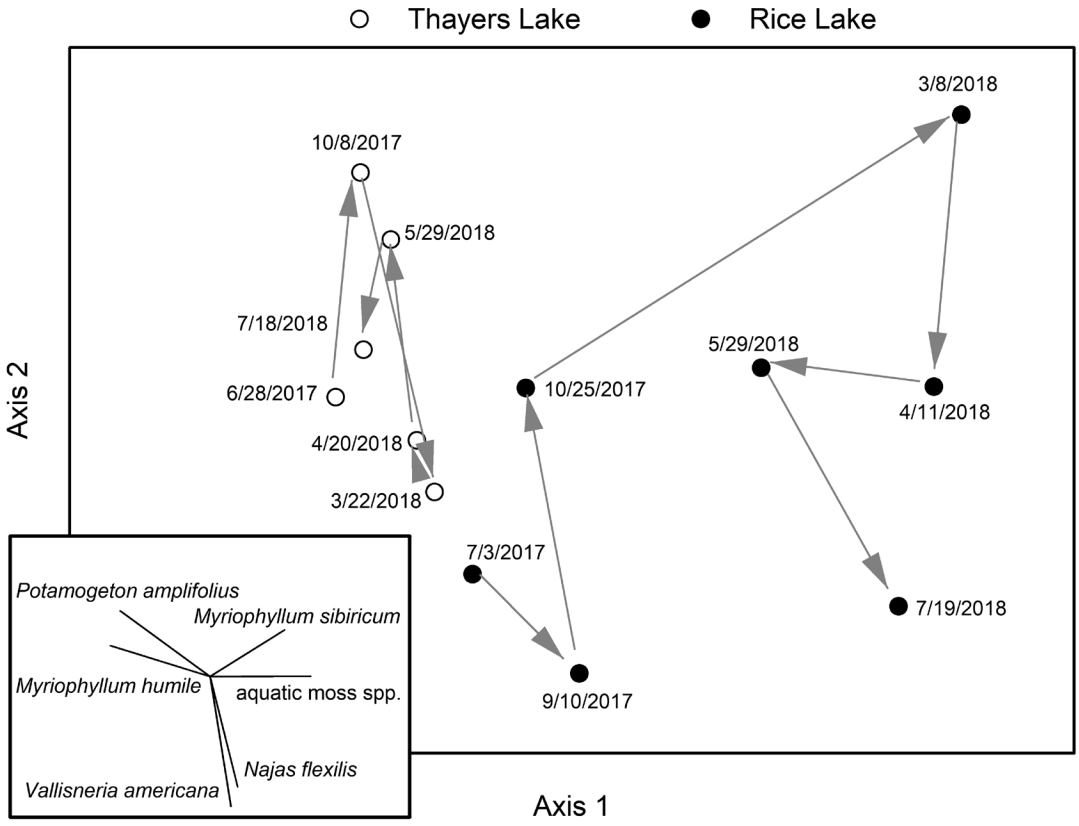

Figure 2.4: NMS ordination of plots in species space. Plots are depicted as circles for each respective waterbody and gray arrows indicate successional vectors between plots at sampled timepoints (plots dated). Inset in the lower left corner is the same NMS ordination with joint plots of macrophyte species variables (r^2 cutoff = 0.30). Macrophytes species explaining ordination space are *Potamogeton amplifolius* (Axis 1 R^2 = 0.45, Axis 2 R^2 = 0.23), *Myriophyllum sibiricum* (Axis 1 R^2 = 0.37, Axis 2 R^2 = 0.17), aquatic moss spp. (Axis 1 R^2 = 0.50, Axis 2 R^2 = 0.00), *Najas flexilis* (Axis 1 R^2 = 0.14, Axis 2 R^2 = 0.39), *Vallisneria americana* (Axis 1 R^2 = 0.10, Axis 2 R^2 = 0.46), and *M. humile* (Axis 1 R^2 = 0.50, Axis 2 R^2 = 0.11) (Appendix J).

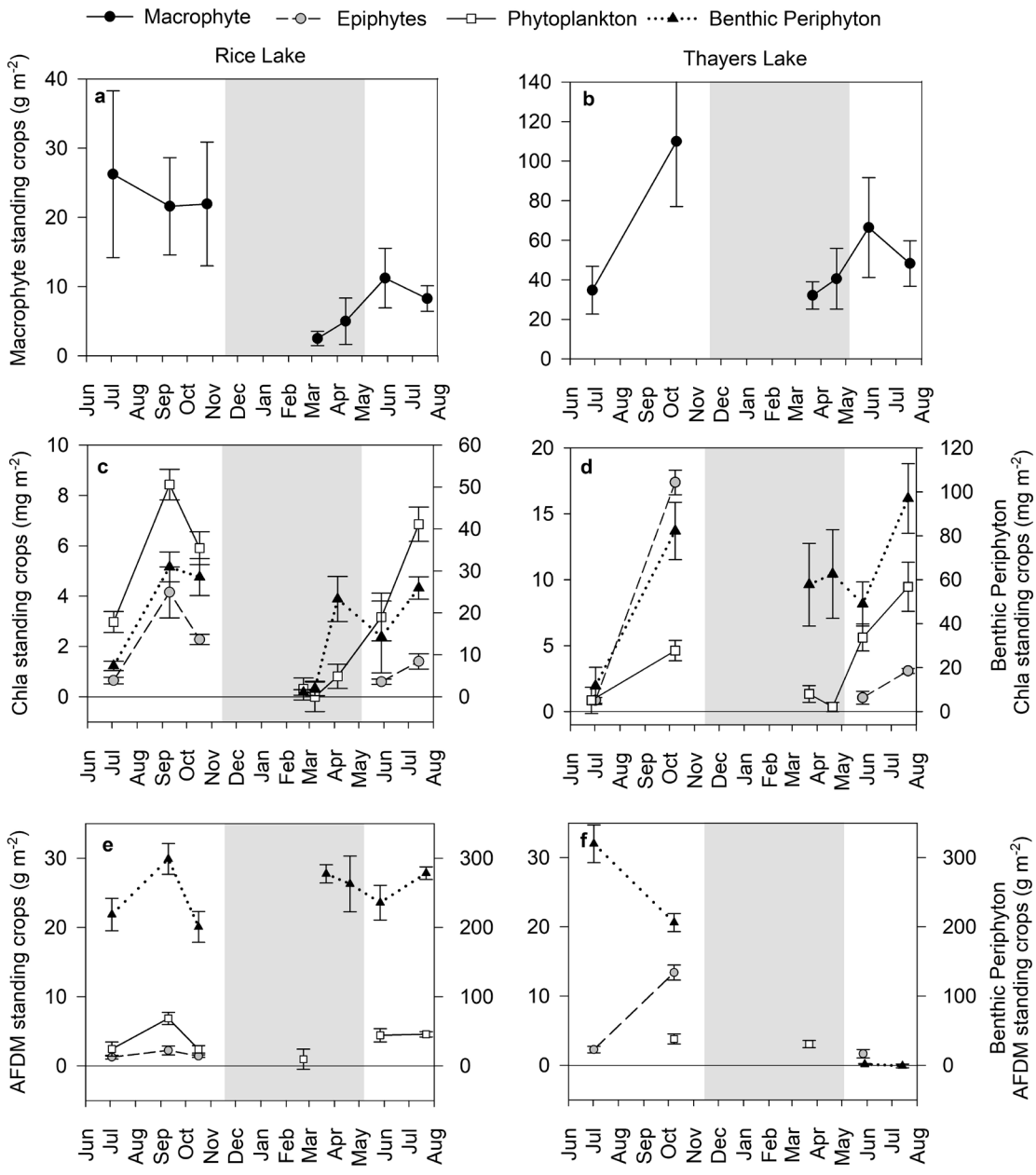

Figure 2.5: Standing crops of epiphytes, phytoplankton, benthic periphyton, and macrophytes on sample dates from 2017-2018. Benthic periphyton values are graphed on the secondary y-axis for Chla and ash free dry mass (AFDM) standing crop. The shaded background indicates when lakes had ice cover.

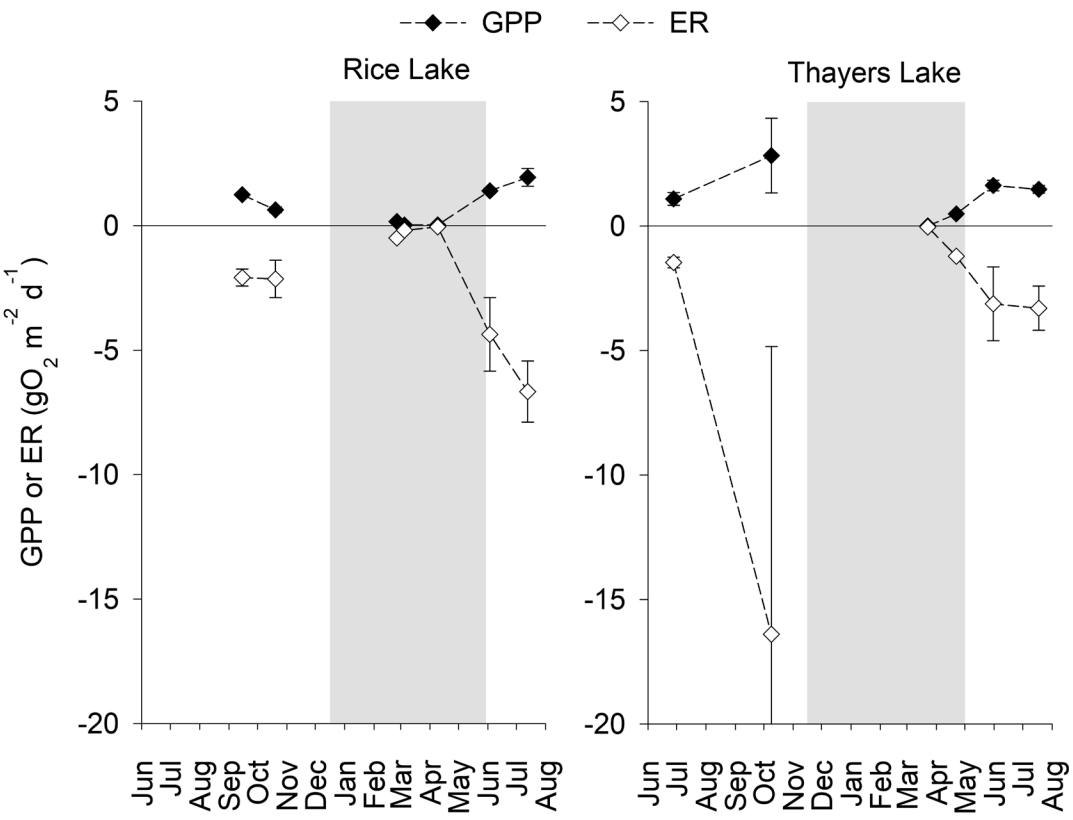

Figure 2.6: Open water metabolism rates of GPP and ER in Rice and Thayers Lake from 2017 to 2018. The shaded background indicates when lakes had ice cover.

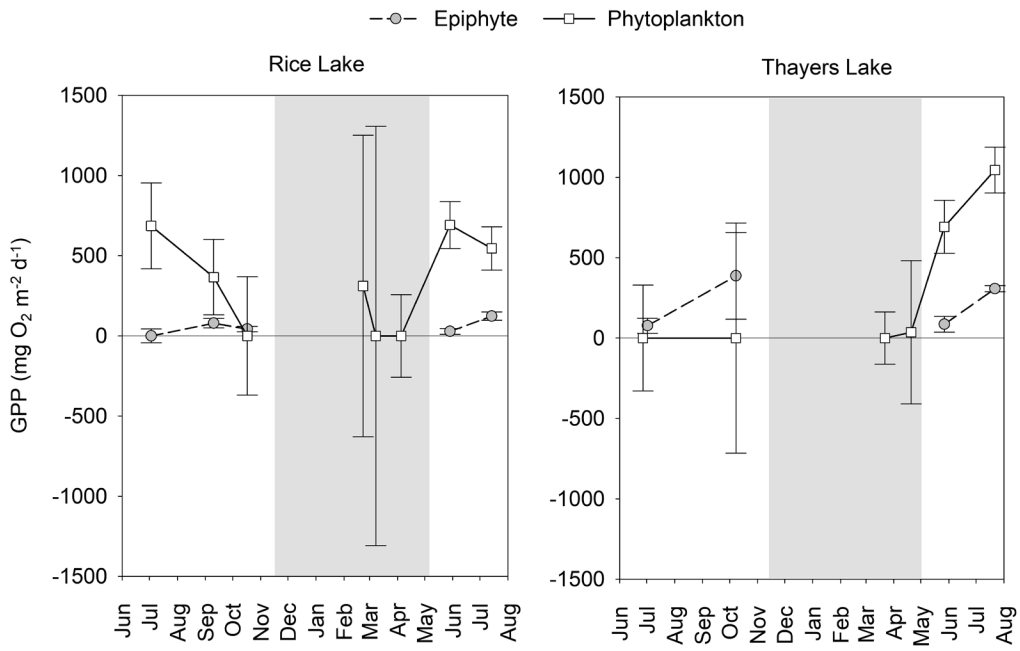

Figure 2.7: GPP rates of epiphytes and phytoplankton on sample dates from 2017-2018. The shaded background indicates when lakes had ice cover.

A Appendix

Appendix A: Water characteristics and nutrients of uninvaded (UNINV) and invaded (INV) plots in Chapter 1

Plot	Light extinction coefficient	Water temperature (°C)	Conductivity (mS cm^{-1})	TDN (mg/l)	DOC (mg/l)	NO_3^-+NO_2^- (µg/l)	NH_4^+ (µg/l)	SRP (µg/l)
HSL-UNINV	0.563	23.91	0.244	0.444	7.27	6.0	18.11	0.89
HSL-INV	0.612	22.31	0.243	0.446	7.48	1.6	24.08	0.89
STHL-UNINV	1.277	22.37	0.179	0.542	14.89	9.0	9.89	0.89
STHL-INV	1.190	22.14	0.179	0.577	14.32	1.6	16.80	11.10
LCI-UNINV	0.395	20.67	0.208	0.187	3.05	30.0	8.46	0.89
LCI-INV	0.366	20.35	0.209	0.218	3.21	71.0	6.72	2.00
SLG-UNINV	1.545	18.21	0.125	0.305	9.15	4.0	1.84	0.89
SLG-INV	0.989	18.98	0.124	0.342	9.17	46.0	3.99	3.10
IRL-UNINV	1.647	20.32	0.074	0.523	13.33	5.0	26.92	0.89
IRL-INV	0.990	20.83	0.073	0.533	11.89	6.0	12.00	0.89
TCH-UNINV	1.050	20.15	0.150	0.418	8.05	14.0	7.32	0.89
TCH-INV	0.882	20.99	0.149	0.259	6.70	71.0	7.64	8.10

Appendix B: Matrix of macrophyte species standing crops (g m^{-2}) at study plots in Chapter 1

	Species																							
Plots	*Utricularia macrorhiza*	*Chara* spp.	*P. richardsonii*	*Ceratophyllum demersum*	*Ranunculus flammula*	*Vallisneria americana*	*Elodea canadensis*	IWM	*P. robbinsii*	*P. zosteriformis*	*Isoetes lacustris*	*P. amplifolius*	*P. oakesianus*	*P. perfoliatus*	*Stuckenia pectinata*	*Najas flexilis*	*P. pusillus spp.*	*Najas guadalupensis*	*Isoetes tenella*	*P. gramineus*	*P. vaseyi*	*Ranunculas aquatilis*	*Bidens becki*	*Heternthera dubia*	*Nymphaea odorata*
HSL-INV	0	0.36	0	0	0	0	0	20.55	0	1.12	0	0	1.03	0	0	1.09	0	0.04	0	0.37	0	0	0	0	0
STHL-INV	0	6.28	0	0	0	0	28.98	67.93	84.15	4.14	0	0	0	1.5	0	0	0	3.43	0	0	0	0	0	0	0
TCH-INV	0	0	0	0	0	7.77	2.47	154.57	0	4.75	0	0	0	0	0.49	0	0.19	0	0	1.83	0	0	0.75	0	0
SLG-INV	0.56	13.45	2.42	1.09	0	63.99	17.09	45.47	0	0	0	0	0	0	0	0	0	0	0	0	0.82	0.16	23.41	1.39	0
LCI-INV	0	3.63	0	0.69	0	25.14	3.26	87.23	0	8.59	0	0	0	0	0	6.18	0	0	0	0.48	0	0	0	0	0
IRL-INV	0	0	0	0	0	0	0	164.27	64.99	0	0	10.74	0	0	0	0	0	0	0	0	0	0	0	0	0
HSL-NAT	0	109.59	0.77	0	0	0	0	5.27	0	2.66	0	0	0	0	0	0.13	0	1.97	0	0	0	0	0	0	0
STHL-NAT	0.01	0	0	0	0	0.14	0.16	1.04	294.73	0	0	0	0	0	0	0	0	0	0	9.75	0	0	1.52	0	0.39
TCH-NAT	0	0.03	0	0.03	0.31	7.38	0	0	0	0	0.43	0	0	0	0	0.05	0	0	0.8	6.48	0	0	0.13	0	0
SLG-NAT	0	2.18	8.11	0.31	0	120.82	0.3	0	0	0	0	0	0	0	0	0.14	0	0	0	0	0	0	0.37	0.01	0
LCI-NAT	0	2.18	0	0	0	1.83	0	0	0	0	0	0	0	0	0	28.47	0	0	0	121.54	0	0	0	0.06	0
IRL-NAT	0	2.54	0	0	0	0	0	4.34	15.96	0	0	60.62	0	0	0	0	0	0	0	0	0	0	0	0	0

P. = Potamogeton

Appendix C: Reduced and logarithmic transformed matrix of macrophyte species used for NMS ordination analysis in Chapter 1

	Species														
Plots	*Utricularia macrorhiza*	*Chara* spp.	*P. richardsonii*	*Ceratophyllum demersum*	*Vallisneria americana*	*Elodea canadensis*	IWM	*P. robbinsii*	*P. zosteriformis*	*P. amplifolius*	*Najas flexilis*	*Najas guadalupensis*	*P. gramineus*	*Bidens becki*	*Heternthera dubia*
HSL-INV	0	2.56	0	0	0	0	4.31	0	3.05	0	3.04	1.57	2.56	0	0
STHL-INV	0	3.78	0	0	0	4.46	4.83	4.93	3.62	0	0	3.54	0	0	0
TCH-INV	0	0	0	0	3.89	3.39	5.19	0	3.68	0	0	0	3.26	2.88	0
SLG-INV	2.75	4.12	3.38	3.04	4.81	4.23	4.66	0	0	0	0	0	0	4.37	3.14
LCI-INV	0	3.56	0	2.84	4.40	3.51	4.94	0	3.93	0	3.79	0	2.69	0	0
IRL-INV	0	0	0	0	0	0	5.22	4.81	0	4.03	0	0	0	0	0
HSL-NAT	0	5.04	2.89	0	0	0	3.72	0	3.43	0	2.13	3.30	0	0	0
STHL-NAT	0.81	0	0	0	2.14	2.14	3.02	5.47	0	0	0	0	3.99	3.18	0
TCH-NAT	0	1.53	0	1.48	3.87	0	0	0	0	0	1.71	0	3.81	2.11	0
SLG-NAT	0	3.34	3.91	2.50	5.08	2.47	0	0	0	0	2.15	0	0	2.56	1.15
LCI-NAT	0	3.34	0	0	3.26	0	0	0	0	0	4.45	0	5.08	0	1.77
IRL-NAT	0	3.40	0	0	0	0	3.64	4.20	0	4.78	0	0	0	0	0

P. = Potamogeton

Logarithmic transformation follows this equation $b_{ij} = \log_{10}\left(x_{ij} + \log^{-1}(\mathrm{Int}(\log(\mathrm{Min}(x))))\right) - (\mathrm{Int}(\log(\mathrm{Min}(x)))$ where: Min(*x*) is the smallest nonzero value in the data and Int(*x*) is a function that truncates *x* to an integer with no decimal places (McCune and Grace 2002).

Appendix D: Diversity indices of the macrophyte assemblages for uninvaded (UNINV) and invaded (INV) plots in Chapter 1

Plot	Species richness	Evenness	Shannon's diversity index	Simpson's diversity index
HSL-UNINV	6	0.23	0.44	0.18
HSL-INV	7	0.36	0.70	0.30
STHL-UNINV	8	0.10	0.21	0.08
STHL-INV	7	0.63	1.32	0.67
LCI-UNINV	5	0.38	0.62	0.34
LCI-INV	8	0.55	1.15	0.54
SLG-UNINV	8	0.18	0.37	0.16
SLG-INV	11	0.67	1.61	0.75
IRL-UNINV	4	0.58	0.81	0.43
IRL-INV	3	0.69	0.75	0.46
TCH-UNINV	9	0.52	1.13	0.60
TCH-INV	8	0.24	0.50	0.20

Appendix E: Pairwise comparison of variables for stepwise multiple linear regressions in Chapter 1. Pearson correlations (*r*) are on the lower left and *p* values listed are gray on the upper right shaded in grey for each pairwise comparison. Significant collinearity was determined as $p \leq 0.05$ (bold)

	Light extinction	Water temperature	Conductivity	TDN	DOC	$NO_3^- + NO_2^-$ †	NH_4^+ †	Macrophyte standing crop	Benthic periphyton Chla†	Epiphyte Chla†	Phytoplankton Chla†	Benthic periphyton AFDM†	Epiphyte AFDM†	Phytoplankton AFDM†	Benthic periphyton GPP	Epiphyte GPP†	Phytoplankton GPP	GPP plot†	ER plot†‡
Light extinction	*	0.25	**0.01**	0.08	0.00	0.17	0.70	0.65	0.56	0.89	0.09	0.20	0.35	0.86	0.35	0.68	0.51	0.82	0.92
Water temperature	-0.36	*	**0.04**	0.15	0.66	0.22	**0.01**	0.70	0.23	0.34	0.19	0.45	0.40	0.04	0.21	0.36	**0.01**	0.95	0.06
Conductivity	-0.72	0.61	*	0.45	0.11	0.97	0.51	0.54	0.53	0.31	0.22	0.27	0.73	0.20	0.08	0.46	0.32	0.72	0.32
TDN	0.52	0.45	-0.24	*	**0.00**	**0.01**	**0.05**	0.54	0.99	0.27	**0.00**	0.74	0.14	0.11	0.99	0.14	0.09	0.90	0.25
DOC	0.79	0.14	-0.49	0.88	*	**0.05**	0.39	0.17	0.42	0.55	**0.00**	0.87	0.21	0.42	0.39	0.37	0.58	0.86	0.44
$NO_3^- + NO_2^-$ †	-0.43	-0.38	-0.01	-0.71	-0.58	*	0.13	0.71	0.35	0.22	0.13	0.17	0.10	0.11	0.40	0.23	0.05	0.57	0.46
NH_4^+ †	-0.12	0.75	0.21	0.58	0.27	-0.46	*	0.64	0.07	0.32	0.09	0.89	0.24	0.22	0.32	0.22	**0.01**	0.17	0.63
Macrophyte standing crop	0.15	0.13	-0.20	0.20	0.43	0.12	-0.15	*	**0.03**	0.19	0.17	**0.05**	0.38	0.96	**0.04**	0.20	0.59	0.32	0.74
Benthic periphyton Chla†	-0.19	0.37	0.20	0	-0.25	-0.29	0.54	-0.61	*	0.65	0.94	0.06	0.65	0.80	**0.05**	0.73	0.74	0.23	0.76
Epiphyte Chla†	-0.04	-0.30	-0.32	-0.34	-0.19	0.38	-0.31	0.40	-0.15	*	0.65	0.53	**0.00**	**0.04**	0.25	**0.00**	0.07	0.35	0.04
Phytoplankton Chla†	0.51	0.41	-0.38	0.80	0.80	-0.47	0.51	0.42	0.03	-0.15	*	0.75	0.28	0.33	0.22	0.49	0.31	0.44	0.30
Benthic periphyton AFDM†	-0.40	0.24	0.34	-0.11	-0.05	0.43	0.05	0.58	-0.56	0.20	-0.10	*	0.42	0.78	0.52	0.58	0.49	0.78	0.85
Epiphyte AFDM†	-0.30	-0.27	-0.11	-0.45	-0.39	0.50	-0.37	0.28	-0.15	0.92	-0.34	0.26	*	**0.03**	0.40	**0.00**	0.08	0.42	0.10
Phytoplankton AFDM†	-0.06	0.60	0.40	0.49	0.26	-0.49	0.38	-0.02	0.08	-0.60	0.31	-0.09	-0.62	*	0.27	**0.02**	**0.01**	0.73	0.08
Benthic periphyton GPP	-0.30	0.39	0.53	0	-0.27	-0.27	0.31	-0.61	0.57	-0.36	-0.38	-0.21	-0.27	0.34	*	0.32	0.08	0.64	0.32
Epiphyte GPP†	-0.13	-0.29	-0.24	-0.45	-0.29	0.37	-0.38	0.40	-0.11	0.95	-0.22	0.18	0.91	-0.67	-0.32	*	0.09	0.41	0.13
Phytoplankton GPP	-0.21	0.71	0.32	0.51	0.18	-0.57	0.70	-0.18	0.53	-0.54	0.32	-0.22	-0.52	0.71	0.53	-0.51	*	0.80	0.07
GPP plot†	-0.07	-0.02	0.12	0.04	0.06	-0.18	-0.43	0.32	-0.37	0.15	-0.25	0.09	0.26	0.11	0.15	0.26	0.08	*	0.39
ER plot†‡	0.03	-0.56	-0.31	-0.36	-0.25	0.24	-0.16	-0.11	-0.10	0.59	-0.33	0.06	0.50	-0.53	-0.32	0.47	-0.54	-0.27	*

Chla = chlorophyll a
AFDM = ash free dry mass
GPP = gross primary productivity
ER = ecosystem respiration
† log transformed
‡ Converted to positive values from negative values
* Not applicable

Appendix F: Correlations of macrophyte species with NMDS ordination axes in Chapter 1

	Axis 1		Axis 2		Axis 3	
Species	*r*	R^2	*r*	R^2	*r*	R^2
Utricularia macrorhiza	-0.09	0.01	0.26	0.07	0.57	0.32
Chara spp.	-0.09	0.01	-0.71	0.50	0.13	0.02
Potamogeton richardsonii	-0.27	0.07	-0.29	0.08	0.54	0.29
Ceratophyllum demersum	-0.54	0.29	0.04	0.00	0.47	0.22
Vallisneria americana	-0.83	0.69	0.29	0.08	0.32	0.10
Elodea canadensis	-0.11	0.01	0.09	0.01	0.86	0.74
Myriophyllum spicatum	0.66	0.44	-0.17	0.03	0.42	0.18
Potamogeton robbinsii	0.77	0.59	0.48	0.23	0.00	0.00
Potamogeton zosteriformis	0.10	0.01	-0.67	0.45	0.26	0.07
Potamogeton amplifolius	0.72	0.51	0.29	0.08	-0.36	0.13
Najas flexilis	-0.57	0.33	-0.51	0.26	-0.49	0.24
Najas guadalupensis	0.35	0.12	-0.69	0.48	0.18	0.03
Potamogeton gramineus	-0.56	0.32	0.27	0.07	-0.46	0.21
Bidens becki	-0.43	0.19	0.52	0.27	0.61	0.37
Heteranthera dubia	-0.39	0.15	0.07	0.01	0.28	0.08

Appendix G: Matrix of macrophyte species standing crops (g m^{-2}) at study plots in Chapter 2

		Species																			
Plots	Date	*Myriophyllum alterniflorum*	Aquatic Moss spp.	*Chara* spp.	*Utricularia macrorhiza*	*Ranunculus flammula*	*Vallisneria americana*	*Utricularia intermedia*	*Spongilla* spp.	*Isoetes lacustris*	*Utricularia purpurea*	*Potamogeton amplifolious*	*Myriophyllum humile*	*Myriophyllum sibiricum*	*Potamogeton epihydrus*	*Elocharis robbinsii*	*Najas flexilis*	*Utricularia minor*	*Potamogeton gramineus*	*Myriophyllum heterophyllum*	*Bidens becki*	*Nyphmaea odorata*
Thayers Lake	7/28/2017	0.29	0	0.04	0	0	0	0	0	0	0	18.58	10.35	0	0	0.25	0	0	2.42	0	0.58	0
Thayers Lake	10/8/2017	0	0	6.41	0	0	0	0	0.77	0	0	66.42	13.66	0	0	5.79	0	0	0	0	9.71	0
Thayers Lake	3/22/2018	0	0	11.18	0	0	0	0	0	0	0	11.28	6.29	0	0	0	0	0	0	0	1.31	0
Thayers Lake	4/20/2018	0	0	12.38	0	0	0	0	0	0	0	18.33	7.19	0	0	0	0	0	0	0	0	0
Thayers Lake	5/29/2018	0	0	5.04	0	0	0	0	0	0	0	45.14	3.84	0	0	6.67	0	0	0	0	0.94	0.46
Thayers Lake	7/18/2018	0	0	1.86	0	0	0	0.02	0	0	0	20.48	14.60	0	0	4.35	0	0	0	0	3.79	0
Rice Lake	7/3/2017	0	0	12.24	0	0	0.50	0	0	0	0	10.31	0	0	1.47	0	0	0	0	0	0	0
Rice Lake	9/10/2017	0	0	3.73	0	0	3.76	0	0	0.04	2.61	6.68	0	0	0	0	0.05	0	0	3.32	0	0
Rice Lake	10/25/2017	0	1.03	1.87	0	0	0	0	0	0.23	0	17.37	0	0	0	0	0	0	0	0	0	0
Rice Lake	3/8/2018	0	1.09	0.20	0	0	0	0.55	0	0	0	0.03	0	0.49	0	0	0	0	0	0	0	0
Rice Lake	4/11/2018	0	3.73	0.85	0	0	0	0	0	0.11	0	0	0	0	0	0	0	0	0	0	0	0
Rice Lake	5/29/2018	0	5.35	1.32	0	0.10	0	0	0	0.75	0	2.94	0	0	0	0	0	0.02	0	0	0	0
Rice Lake	7/19/2018	0	2.13	0.78	0.29	0	4.17	0	0	0.07	0	0.05	0	0.14	0	0	0.09	0	0	0	0	0

Appendix H: Diversity indices of the macrophyte assemblages for uninvaded (UNINV) and invaded (INV) plots in Chapter 2

Plot	Date	Species richness	Evenness	Shannon's diversity index	Simpson's diversity index
Thayers Lake	7/28/2017	7	0.53	1.04	0.57
Thayers Lake	10/8/2017	6	0.64	1.15	0.55
Thayers Lake	3/22/2018	4	0.87	1.20	0.68
Thayers Lake	4/20/2018	3	0.94	1.03	0.62
Thayers Lake	5/29/2018	6	0.53	0.95	0.45
Thayers Lake	7/18/2018	6	0.72	1.29	0.67
Rice Lake	7/3/2017	5	0.60	0.96	0.57
Rice Lake	9/10/2017	7	0.81	1.58	0.78
Rice Lake	10/25/2017	4	0.40	0.56	0.27
Rice Lake	3/8/2018	5	0.80	1.28	0.68
Rice Lake	4/11/2018	3	0.53	0.58	0.33
Rice Lake	5/29/2018	6	0.67	1.21	0.64
Rice Lake	7/19/2018	8	0.60	1.24	0.62

Appendix I: Pairwise comparison of variables for stepwise multiple linear regressions in Chapter 2. Pearson correlations (*r*) are on the lower left and *p* values listed are gray on the upper right shaded in grey for each pairwise comparison. Significant collinearity was determined as $p \leq 0.05$ (bold)

	% light at 1m depth	Light extinc-tion	Water tem-pera-ture	Con-ductiv-ity†	NH_4^+†	Macro-phyte stand-ing crop†	Phyto-plank-ton Chla†	Epi-phyte Chla†	Benthic periph-yton Chla†	Phyto-plank-ton AFDM†	Epi-phyte AFDM†	Benthic periph-yton AFDM	Phyto-plank-ton GPP	Epi-phyte GPP	Plot GPP	Plot ER†
% light at 1m depth	*	0.54	**0.00**	0.19	0.07	0.11	**0.00**	0.56	0.16	0.25	0.68	0.10	0.24	0.63	**0.01**	**0.00**
Light extinction	0.20	*	0.17	0.46	0.37	0.84	0.26	0.60	0.41	0.10	0.41	0.40	0.24	0.65	0.28	0.24
Water temperature	0.88	0.42	*	**0.00**	**0.02**	0.53	**0.01**	0.09	0.75	0.81	0.18	0.41	0.08	0.50	**0.00**	**0.00**
Conductivity†	-0.46	-0.26	-0.80	*	**0.04**	0.58	0.30	**0.01**	0.28	0.71	0.19	0.71	0.80	**0.05**	0.33	0.27
NH_4^+†	-0.54	0.28	-0.60	0.62	*	0.34	0.31	0.75	0.56	0.91	0.95	0.86	0.26	0.75	0.17	0.15
Macrophyte standing crop†	0.51	0.07	0.19	0.20	-0.29	*	0.70	0.13	**0.01**	0.51	**0.01**	0.40	0.17	0.08	0.07	0.11
Phytoplankton Chla†	0.79	0.37	0.71	-0.37	-0.31	0.13	*	0.22	0.10	0.14	0.91	0.36	0.33	0.39	**0.02**	**0.05**
Epiphyte Chla†	0.27	-0.24	-0.60	0.92	0.12	0.54	0.45	*	**0.02**	0.19	**0.01**	0.58	0.46	**0.01**	0.14	0.16
Benthic periphyton Chla†	0.44	-0.26	0.09	0.36	-0.17	0.72	0.48	0.76	*	**0.04**	0.12	0.12	0.33	**0.00**	0.10	0.31
Phytoplankton AFDM†	0.40	-0.55	0.08	0.14	-0.04	0.23	0.48	0.56	0.61	*	0.15	**0.04**	0.87	0.34	0.43	0.77
Epiphyte AFDM†	0.19	-0.37	-0.49	0.62	-0.02	0.83	0.04	0.83	0.56	0.60	*	0.69	0.40	0.03	0.18	0.38
Benthic periphyton AFDM	0.49	-0.27	0.24	0.13	-0.05	0.25	0.28	-0.21	0.44	0.60	-0.15	*	0.45	0.90	0.41	0.47
Phytoplankton GPP	0.36	0.37	0.49	-0.09	-0.32	0.40	0.30	-0.29	0.28	-0.05	-0.32	0.22	*	0.93	0.10	0.14
Epiphyte GPP	0.23	-0.21	-0.26	0.81	-0.13	0.60	0.33	0.82	0.85	0.42	0.72	-0.05	0.04	*	**0.03**	0.07
Plot GPP	0.76	0.36	0.75	-0.32	-0.41	0.54	0.66	0.57	0.48	0.27	0.53	0.25	0.47	0.74	*	**0.00**
Plot ER‡†	0.78	0.38	0.78	-0.32	-0.42	0.48	0.57	0.55	0.31	0.10	0.36	0.22	0.43	0.67	0.89	*

Chla = chlorophyll a
AFDM = ash free dry mass
GPP = gross primary productivity
ER = ecosystem respiration
† log transformed
‡ Converted to positive values from negative values
* Not applicable

Appendix J: Correlations of macrophyte species with NMDS ordination axes in Chapter 2

	Axis 1		Axis 2	
Species	*r*	R^2	*r*	R^2
Myriophyllum alterniflorum	-0.30	0.09	0.01	0
Aquatic Moss spp.	0.71	0.50	0.03	0
Chara spp.	-0.50	0.25	-0.26	0.07
Utricularia macrorhiza	0.42	0.18	-0.38	0.14
Ranunculus flammula	0.24	0.06	0.06	0
Vallisneria americana	0.32	0.10	-0.68	0.46
Utricularia intermedia	0.49	0.24	0.53	0.28
Spongilla spp.	-0.27	0.07	0.42	0.18
Isoetes lacustris	0.33	0.11	0.01	0
Utricularia purpurea	0.01	0	-0.50	0.25
Potamogeton amplifolious	-0.67	0.45	0.48	0.23
Myriophyllum humile	-0.71	0.50	0.33	0.11
Myriophyllum sibiricum	0.61	0.37	0.41	0.17
Potamogeton epihydrus	-0.13	0.02	-0.32	0.10
Elocharis robbinsii	-0.49	0.24	0.53	0.29
Najas flexilis	0.37	0.14	-0.63	0.39
Utricularia minor	0.24	0.06	0.06	0
Potamogeton gramineus	-0.3	0.09	0.01	0
Myriophyllum heterophyllum	0.01	0	-0.50	0.25
Bidens becki	-0.43	0.19	0.45	0.20
Nyphmaea odorata	-0.23	0.05	0.30	0.09